Electronic Supplementary Material (ESI) for ChemComm.

Electronic Supplementary Information

Diels-Alder Cycloaddition Polymerization for Porous Poly-phenylenes with Exceptional Gas Uptake Properties

Timur Ashirov,[1] Patrick W. Fritz,[1] Taner Yildirim[2]* and Ali Coskun[1]*

[1] Department of Chemistry, University of Fribourg, Chemin du Musée 9, 1700 Fribourg, Switzerland

E-mail: ali.coskun@unifr.ch

[2] NIST Center for Neutron Research, National Institute of Standards and Technology, Gaithersburg, MD 20899, USA

***Corresponding author:** ali.coskun@unifr.ch

Table of Contents

Materials and Methods:

Materials: We used the chemicals and solvents without additional purification unless otherwise noted. These materials were obtained from various suppliers: 1,4-Dibromobenzene (99%) from Fluorochem, Trimethylsilylacetylene (99%), copper (I) iodide (99%), ethylvinyl ether (98%), 4-dimethylaminopyridine (DMAP, 98%), and elemental sodium (97%) from Acros Chemicals, 1,3,5-Tribromobenzene (98%) and bis(triphenylphosphine)palladium (II) dichloride (99%) from Sigma Aldrich, carbon tetrachloride (HPLC grade) and azobisisobutyronitrile (AIBN, 99%) from Sigma Aldrich, and zinc chloride (98%) from TCI Chemicals. Dry solvents purified through alumina and molecular sieve columns, while acetic acid and other solvents were purchased from Honeywell and Fischer Chemicals. Sodium and potassium carbonate were obtained from Rosch Chemicals, and all air and moisture-sensitive chemicals were stored in a glovebox under an inert atmosphere of Ar. Finally, 1,2,3-trichlorobenzene (TChB) was acquired from Sigma-Aldrich.

Instrumentation: Silica gel column chromatography was conducted utilizing 230–400 mesh silica gel (Silicyl), while thin-layer chromatography was performed using Merck 60 F254 silica/alumina gel plates. FTIR spectra were acquired using a Perkin-Elmer Frontier spectrometer with KBr pellets (Sigma-Aldrich, 99.85%). The TGA was performed on a Mettler-Toledo TGA/DSC 3+ instrument under 50 sccm of N_2 and 50 sccm of air flow, with a heating rate of 5K/min. The XRD patterns were recorded on a STOE STADIP, utilizing a focused Cu Ka1 incident beam from a germanium monochromator equipped with a Mythen1K detector. Liquid ^{1}H and ^{13}C NMR spectra were obtained using Bruker Avance III 400 and 500 MHz instruments, calibrated according to the TMS signal or the deuterated solvent peak. The XPS spectra were recorded on a multi-purpose XPS, Sigma Probe, Thermo VG Scientific, with Monochromatic Al Kα X-ray source. Samples were prepared on an indium foil to minimize charging and to use small sample quantities, with the foil supported on aluminum foil and affixed to the XPS sample holder. High-resolution spectra were deconvoluted using fityk software.[1] Elemental analysis (EA) was performed on a ThermoFischer Flash 2000 analyzer. The 2,5-Bis(5-tert-butyl-2-benzo-oxazol-2-yl) thiophene (BBOT) was used as a reference standard for the measurements. Solid-state CP-MAS NMR spectra were obtained on a Bruker Avance Neo 600 MHz instrument, with samples spun at 60.0 kHz and a relaxation delay of 5.0 s. Pore size distribution was determined using SAIEUS software, applying non-local density functional theory.[2] FE-SEM were recorded using a ThermoFischer Scios 2 instrument, with an accelerating voltage of 3.0 kV and a current of 0.40 nA. Prior to imaging, all samples were sputtered with 3.5 nm of gold using a Cressington 208HR instrument to mitigate charging effects.

Volumetric high pressure gas sorption measurements: High-pressure gas sorption measurements were performed on an activated samples at the NIST Center for Neutron Research (NCNR) using a computer-controlled Sieverts apparatus. Prior to the sorption study, 250 mg sample was activated under a dynamic vacuum at 150 °C for 12 hours. After each measurement, the sample was heated to 323K and pumped for couple of hours. Volumetric gas adsorption measurements were performed using a custom developed fully computer-controlled Sieverts apparatus as discussed in detail earlier.[3, 4] Briefly, the fully computer-controlled Sievert apparatus operates in a sample temperature range of 20 K to 500 K and a pressure range of 0 to 120 bar. In the volumetric method, gas

is admitted from a dosing cell with known volume to the sample cell in a controlled manner; the gas pressure and temperature are controlled and recorded.

Some unique features of the setup are as follows; The pressure points were chosen on a non-uniform grid such that we have two dozen of points between 0-2 bar range. Hence out high-pressure isotherms can be also considered low pressure isotherms to get Q_{st} at initial loadings. The instrument has five gas inlets including He, H_2, N_2, CO_2, and CH_4, which enables the first nitrogen pore volume and surface measurements followed by He-cold volume determination and finally the gas adsorption measurements without needing to move the sample from the cell. Two high precision pressure gauges with parts-per-billion resolution and typical accuracy of 0.025% (20 psia and 3000 psia, respectively) were used to precisely measure the pressure. For isotherm measurements below room temperature, the sample temperature was controlled using a closed cycle refrigerator (CCR). The difference between the real sample temperature and the control set-point is within 1 K in the whole operating temperature range. The connection between the sample cell and the dose cell is through 1/8" capillary high-pressure tubing, which provided a sharp temperature interface between the sample temperature and the dose temperature (i.e., room temperature). The cold volumes for the empty cell were determined using He as a function of pressure at every temperature before the real sample measurement and were used to calculate the sample adsorption.

Since the adsorbed amount is deducted from the raw P-V-T data using a real gas equation of state, a critically important issue is the accuracy of the chosen equation of state (EOS) in terms of describing the real gas behavior within the desired temperature and pressure range. Using an empty cell as a reference, we found that the MBWR EOS best describes the real gas behavior of He, H_2, CH_4 and CO_2. Therefore, in all our isotherm data reduction, the NIST MBWR EOS is used.

Measured isosteric heat of adsorption Q_{st}: Our isotherm data at multiple temperatures enable us to extract the heat of adsorption Q_{st} as a function of the adsorbed amount. Q_{st} is calculated using the "isosteric method" where a series of isotherms are measured at multiple temperatures. These isotherms are then parameterized by cubic spline which does not require any fitting and allows us to interpolate the isotherm at a constant loading. Then, the Q_{st} is obtained from the ln(P) versus 1/T plots (Figures S11-14). As an alternative to cubic-spline interpolation, we also obtain Q_{st} by fitting the isotherm data using double-site Langmuir model. After the isotherms are fitted, by applying Clausius-Clapeyron equation, the heat of adsorption is obtained from ln(P) versus 1/T plots.

Experimental Procedures for Synthesis of the precursors:

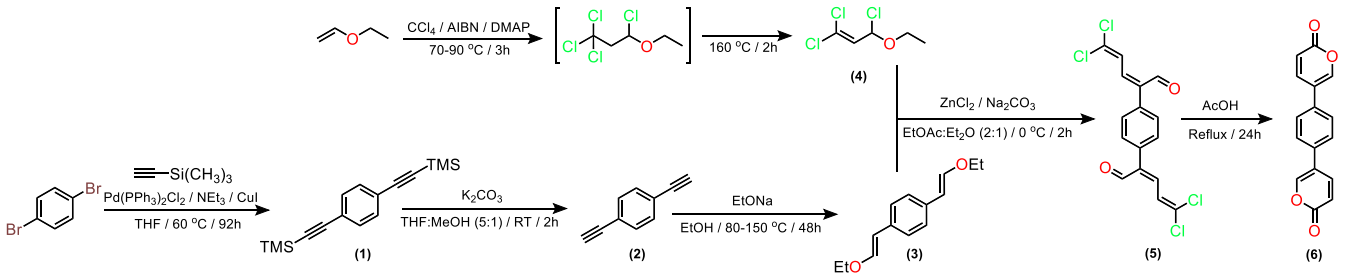

1,4-bis((trimethylsilyl)ethynyl)benzene **(1)**[5-7]:

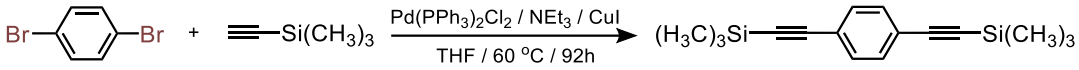

In a 500 mL 3-necked round-bottom flask, a mixture comprising 50.0 grams (0.212 moles, 1.000 equivalent) of 1,4-dibromobenzene (5.0 grams, 7.120 mmol, 0.0336 equivalent), 5.0 gr (0.0071 mol, 0.0336 eq.) of bis(triphenylphosphine)palladium (II) chloride, and copper (I) iodide (4.4 grams, 2.310 mmol, 0.109 equivalent) was prepared. The flask underwent five vacuum-argon backfills before being filled with argon. Subsequently, 250 mL of anhydrous tetrahydrofuran (THF) and 70 mL of triethylamine were introduced, and the mixture was stirred at room temperature for 30 minutes. Next, 84.0 mL (0.607 moles, 2.86 equivalents) of trimethylsilylacetylene were added, causing the solution to darken, and the reaction was heated at 60 °C for 92 hours. After cooling to room temperature, THF was removed under reduced pressure, followed by the addition of 500 mL of water. The organic layer was subjected to extraction with 3x500 mL of CH_2Cl_2 (note: difficult separation) and subsequently dried over $MgSO_4$. Upon evaporation of the solvent under reduced pressure, a black-grey solid was obtained. The mixture was then passed through a 15-20 cm silica plug using heptane at 0 °C, and pure product isolation was achieved through washing with heptane at -20 °C. The purified product was dried at 40 °C, resulting in a yield of 52.1 grams (90.8%) of white powder.

^{1}H NMR (400 MHz, $CDCl_3$) δ 7.38 (s, 4H), 0.24 (s, 18H).

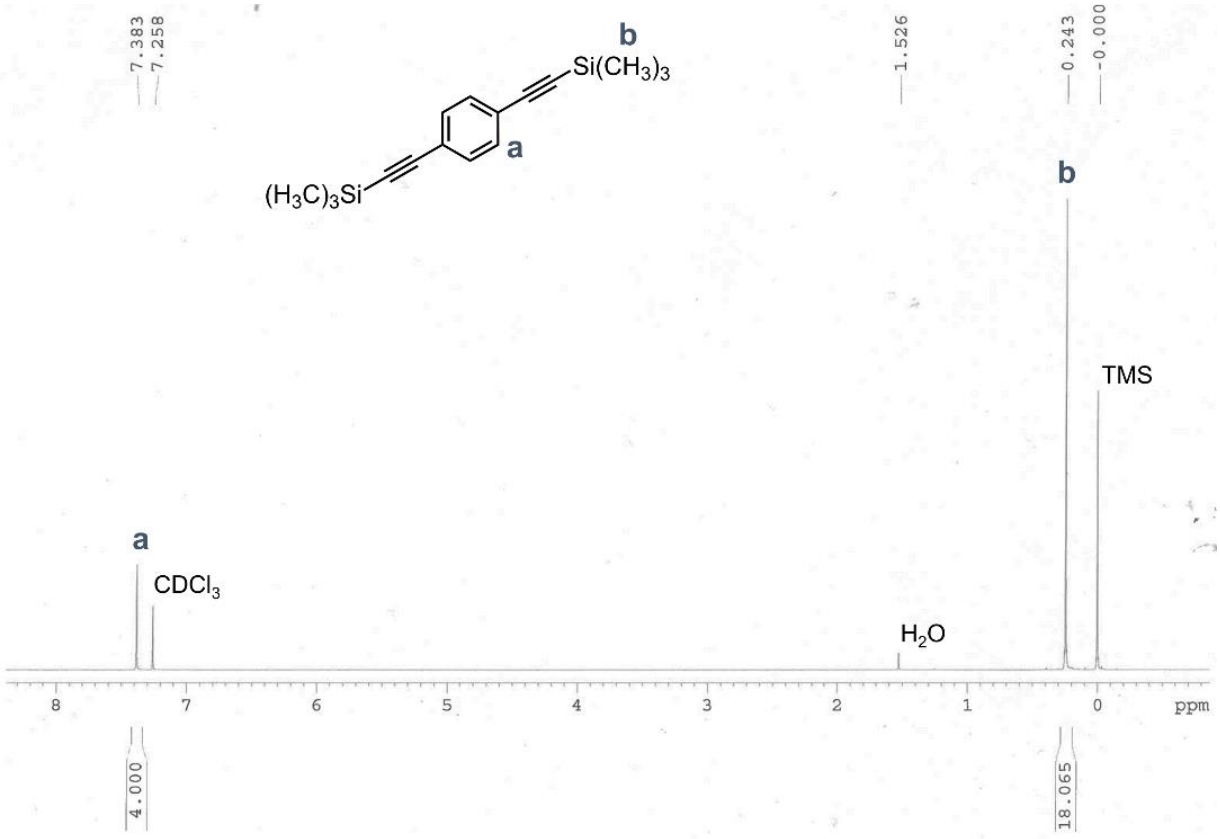

1,4-diethynylbenzene **(2)**[7, 8]:

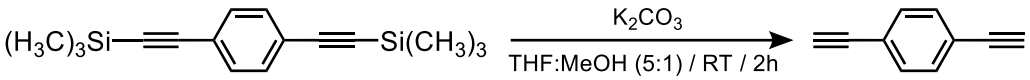

In a 1-liter round-bottom flask, 52.1 grams (0.193 moles, 1.00 equivalent) of 1,4-bis((trimethylsilyl)ethynyl)benzene **(1)** were dissolved in a mixture of 500 mL of tetrahydrofuran (THF) and 100 mL of methanol (MeOH). The solutions exhibited a yellow hue, and 66.5 grams (0.482 moles, 2.50 equivalents) of K_2CO_3 were added. The reaction was stirred at room temperature for 2 hours, causing the color to shift to beige. The reaction mixture was then poured into 500 mL of deionized (DI) water, followed by the evaporation of THF and methanol under reduced pressure, resulting in the formation of a beige-brown precipitate. The mixture was further cooled to 0 °C, the precipitate was filtered, and it was subsequently washed with water. Finally, the product was dried at 40 °C, yielding 21.3 grams (87.6%) of solid product.

^{1}H NMR (400 MHz, $CDCl_3$) δ 7.44 (s, 4H), 3.17 (s, 2H).

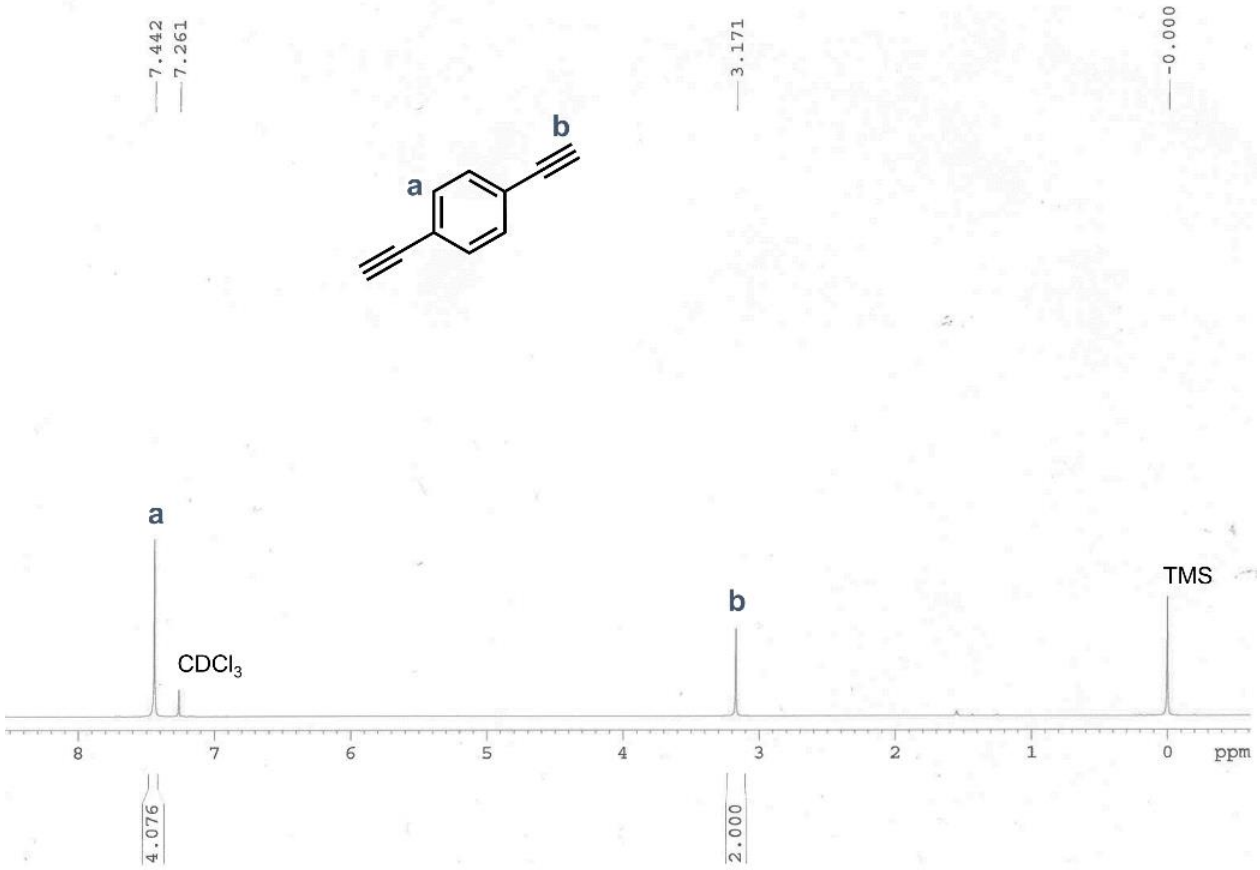

1,1,3-trichloro-3-ethoxyprop-1-ene **(4)**[9-16]:

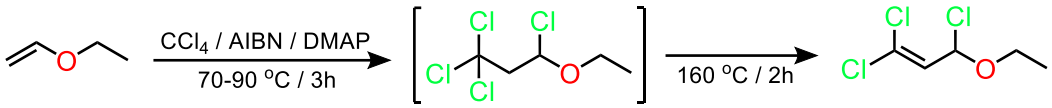

In a 500 mL 3-necked round-bottom flask, a mixture of 154.4 mL (1.60 moles, 2.00 equivalents) of carbon tetrachloride (CCl_4) and 1.3 grams (0.008 moles, 0.01 equivalent) of azobisisobutyronitrile (AIBN) was prepared. To this blend, 76.9 mL (0.800 moles, 1.00 equivalent) of ethylvinyl ether, pre-mixed with 1.5 grams (0.012 moles, 0.015 equivalent) of 4-dimethylaminopyridine (DMAP), was gradually added over a span of 10 minutes. The reaction mixture was then heated to 70 °C and refluxed for 1.5 hours. Subsequently, the temperature was raised to 90 °C, and reflux continued for an additional 2.5 hours, during which the solution transformed to a black color, accompanied by the evolution of hydrogen chloride (HCl). After cooling to room temperature, the mixture was transferred to a 500 mL flask, and excess CCl_4 was removed under reduced pressure, yielding a brown-black sticky oily solution, weighing 161.1 grams. This solution was further heated at 160 °C for 2 hours, during which substantial HCl evolution was observed. After cooling to room temperature, 124.8 grams (41.2%) of black-brown liquid product was separated by decantation and stored at 5 °C. The product containing trace amounts of AIBN, DMAP and 1,1,1,3-tetrachloro-3-ethoxypropane was used without further purification.

^{1}H NMR (400 MHz, $CDCl_3$) δ 6.28 (d, *J*=8 Hz, 1H), 6.23 (d, *J*=8 Hz, 1H), 4.00 (dq, *J*=9.4, 7.1, 1H) 3.61 (dq, *J*=9.4, 7.1, 1H), 1.28 (t, *J*=7.1 Hz, 3H).

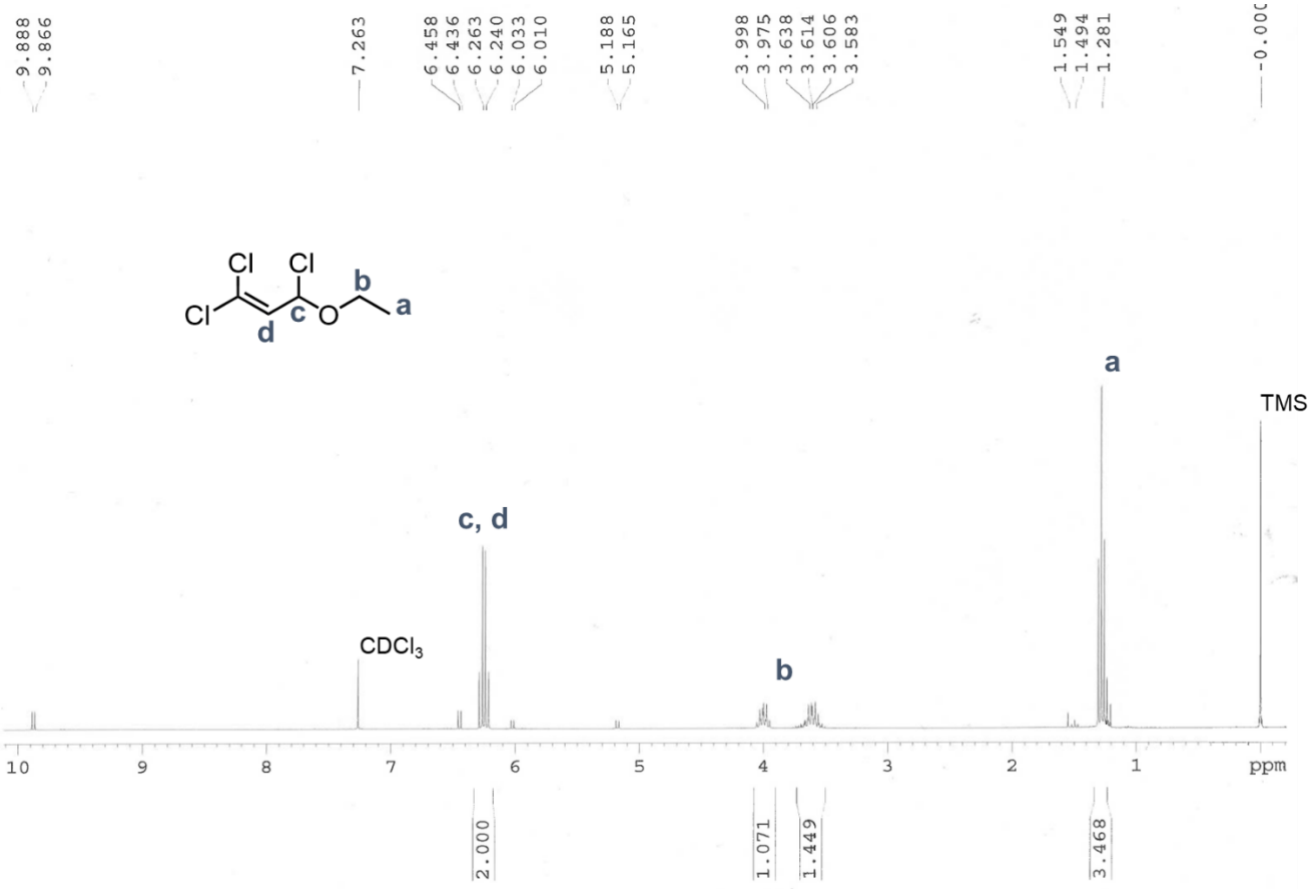

CH_2 protons labelled as “b” are diastereotopic, thus leading to distinct chemical shifts, owing to the chiral center present in “c”.

1,4-bis((E,Z)-2-ethoxyvinyl)benzene **(3)**[15, 17, 18]:

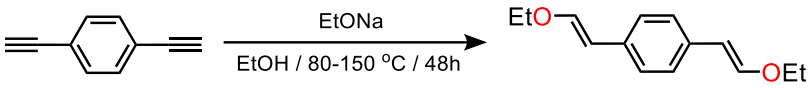

For this procedure, sodium ethoxide (EtONa) was formed *in-situ* by reacting sodium metal and ethanol. Initially, in a 500 mL round-bottom flask, a mixture comprising 217 mL (3.714 moles, 22 equivalents) of ethanol (EtOH) and 15.5 grams (0.675 moles, 4 equivalents) of sodium (Na) was prepared under an argon atmosphere. The mixture was heated to reflux until complete dissolution of sodium was observed. It's worth noting that the mixture needed to be kept warm to prevent the crystallization of EtONa.

Subsequently, in a Pyrex ampule, 21.3 grams (0.169 moles, 1 equivalent) of 1,4-diethynylbenzene **(2)** was placed, and the hot EtONa solution was added and purged with argon. The mixture was kept at 80 °C and stirred until a black-brown solution was formed. The ampule was sealed and then positioned in a preheated oil bath at 150 °C, where it was heated for 48 hours with stirring. Upon cooling to room temperature, a yellow pasty solid material was obtained, which was poured into 1L of ice water mixture. The organic layers were extracted using 3x400 mL of diethyl ether. These organic layers were subsequently washed with 2x300 mL of 0.1M $AgNO_3$ solution and 3x400 mL of deionized (DI) water. Finally, the organic layers were dried over magnesium sulfate ($MgSO_4$), and the solvent was removed under reduced pressure, resulting in the formation of a black-brownish oily liquid. The purified product was obtained through distillation at 150-160 °C under high vacuum, yielding 28.8 grams (78.1%) of pale beige-yellow liquid.

^{1}H NMR (400 MHz, $CDCl_3$) δ 7.52 (s, 4H), 6.17 (d, *J*=7.1 Hz, 2H), 5.19 (d, *J*=7.1 Hz, 2H), 3.97 (q, *J*=7.1 Hz, 4H), 1.36 (t, *J*=7.1 Hz, 6H).

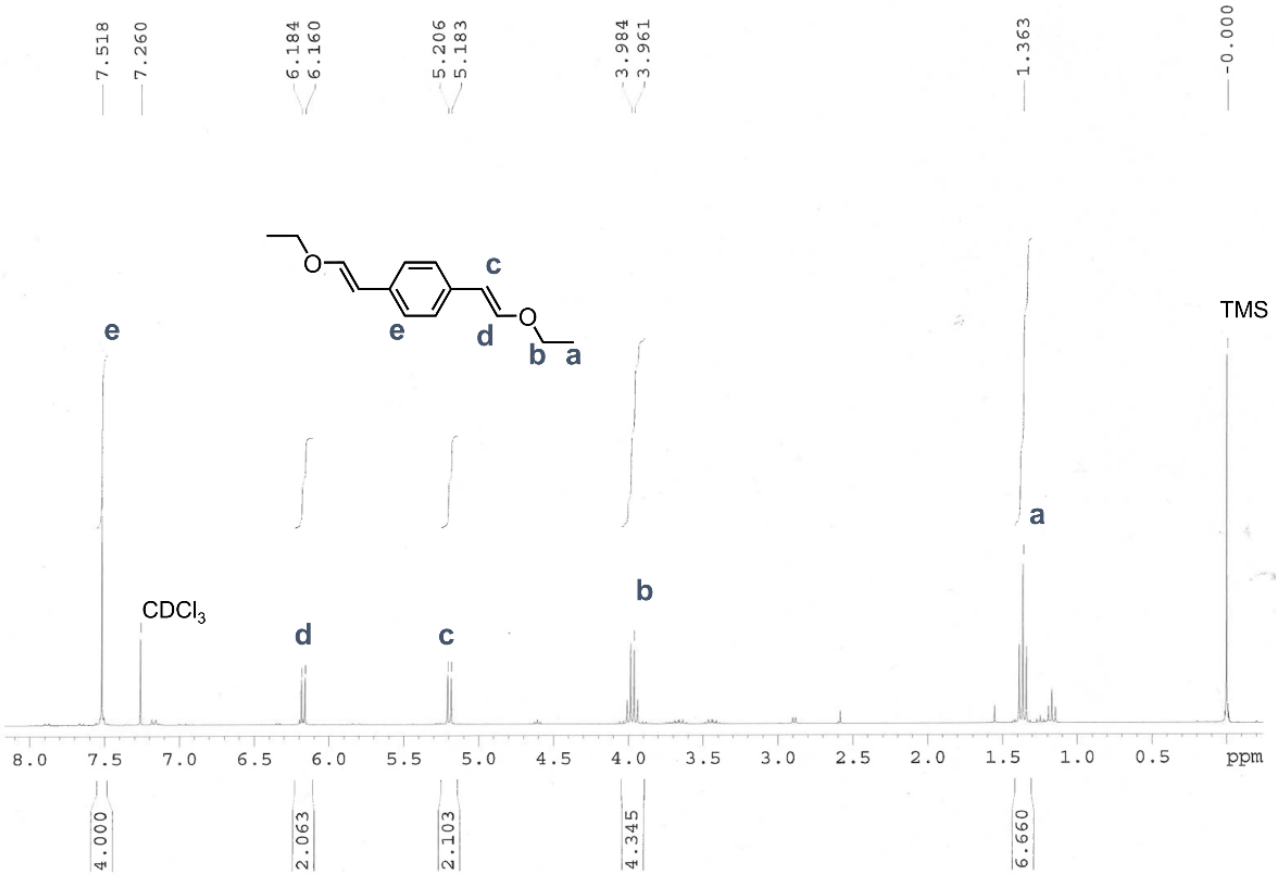

(2Z,2'Z)-2,2'-(1,4-phenylene)bis(5,5-dichloropenta-2,4-dienal) **(5)**[10, 11, 15, 17, 18]:

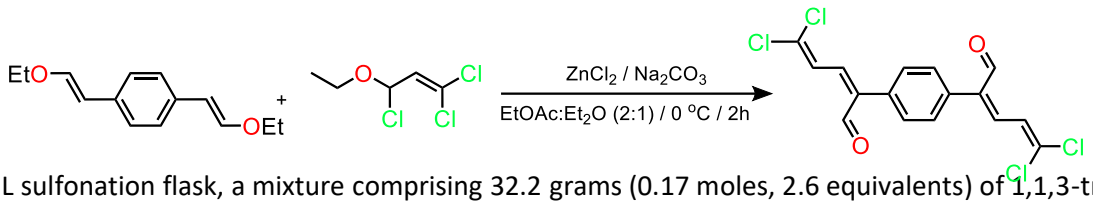

In a 100 mL sulfonation flask, a mixture comprising 32.2 grams (0.17 moles, 2.6 equivalents) of 1,1,3-trichloro-3-ethoxyprop-1-ene **(4)**, 0.8 grams (5.87 mmol, 0.0916 equivalents) of anhydrous zinc chloride ($ZnCl_2$), and 4 mL of dry ethyl acetate (EtOAc) was prepared. The mixture was then cooled to 0 °C, and 14.2 grams (0.065 moles, 1 equivalent) of 1,4-bis((E,Z)-2-ethoxyvinyl)benzene **(3)** was added dropwise over a period of 10 minutes. The reaction was stirred at 0 °C for 1 hour, after which 2.2 grams (0.0208 moles, 0.3 equivalents) of sodium carbonate (Na_2CO_3) were added, and the reaction continued to stir at 0 °C for an additional 30 minutes. Subsequently, 2 mL of anhydrous diethyl ether (Et_2O) were introduced. Solids were removed via filtration, and the filtrate was evaporated, yielding 43.3 grams of brown-black liquid.

To remove excess 1,1,3-trichloro-3-ethoxyprop-1-ene **(4)**, distillation was carried out at 60 °C under high vacuum (10^{-3} mbar). The resulting residue was combined with approximately 850 mL of a ~11% hydrochloric acid (HCl) solution and heated to 50-60 °C for 1 hour and 15 minutes, during which the liquid solidified and began to precipitate. The reaction mixture was then cooled to room temperature and stirred overnight. A crude solid product, amounting to 25.7 grams (~70%), was obtained via filtration, washed with deionized (DI) water, and subsequently used without further purification or characterization.

5,5'-(1,4-phenylene)bis(2H-pyran-2-one) **(6)**[15, 17, 18]:

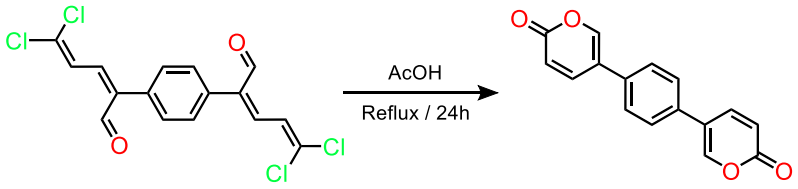

In a 1-liter round-bottom flask, 25.7 grams (0.068 moles, 1 equivalent) of (2Z,2'Z)-2,2'-(1,4-phenylene)bis(5,5-dichloropenta-2,4-dienal) **(5)** was combined with 400 mL of glacial acetic acid. The resulting reaction mixture was refluxed for 24 hours and subsequently cooled down to room temperature, at which point a brown precipitate became formed. These solids were then filtered, washed with a small amount of acetic acid (note that the product was present in the filtrate phase), and 700 mL of deionized (DI) water was introduced to the filtrate. This led to the formation of a yellow-beige precipitate, which was separated via filtration, washed with water, and dried at 40 °C.

The crude product underwent an initial purification step using column chromatography with a solvent gradient of pentane to ethyl acetate (EtOAc) ranging from 4:6 to 3:7. The purified product was subsequently dissolved in 60 mL of diethyl ether (Et_2O), stirred for 30 minutes, and filtered; this operation was repeated twice. Further

purification involved dissolving the product in 200 mL of Et_2O, stirring overnight, and then filtering. This process was repeated three times, with each iteration involving 1 hour of stirring. Finally, the residue was dissolved in 60 mL of ethanol (EtOH), stirred at 60 °C for 1 hour, cooled to room temperature, and filtered. This last step was also performed twice, with the final filtration being carried out with 25 mL of EtOH, ultimately yielding 600 mg (3.3%) of pure product in the form of a beige-brown solid. To enhance the yield, filtrates can be collected, and the aforementioned washing procedure can be reiterated multiple times.

^{1}H NMR (400 MHz, DMSO-d_6) δ 8.30 (dd, *J*=2.8, 1.1 Hz, 2H), 8.05 (dd, *J*=9.8, 2.8 Hz, 2H), 7.68 (s, 4H), 6.50 (dd, *J*=9.7, 1.1 Hz, 2H). ^{13}C NMR (100 MHz, DMSO-d_6) δ 160.5, 149.9, 144.1, 132.6, 126.2, 118.7, 115.5 ppm.

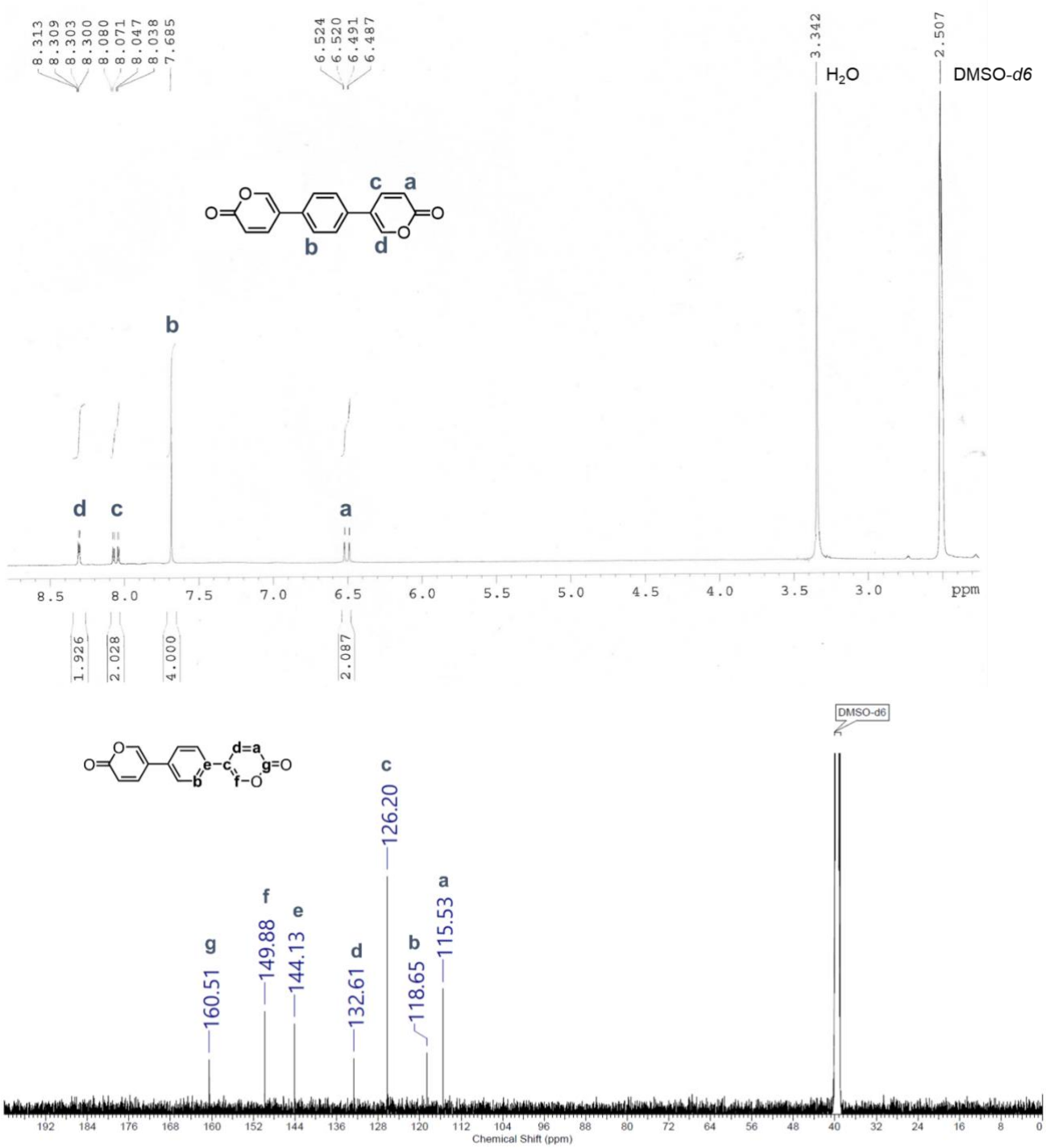

1,3,5-tris((trimethylsilyl)ethynyl)benzene **(8)**[6, 8, 19-21]:

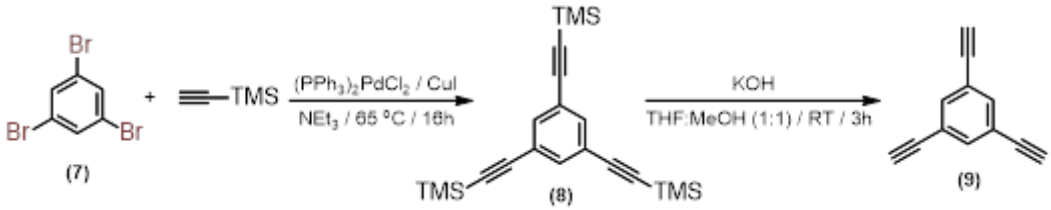

In a 250 mL round-bottom flask, 3.15 grams (0.01 moles, 1 equivalent) of 1,3,5-tribromobenzene, along with 232 milligrams (0.033 mmols, 0.033 eq.) of bis(triphenylphosphine)palladium (II) chloride, 62.8 milligrams (0.033 mmols, 0.033 eq.) of copper (I) iodide, and 50 mL of anhydrous trimethylamine were combined under an argon atmosphere. The resulting reaction mixture was stirred at room temperature for 15 minutes, after which 5.69 mL of trimethylsilylacetylene was added dropwise. The reaction mixture was then heated to 65°C and left to react for 16 hours. Subsequently, it was cooled to room temperature, and 65 mL of hexane was introduced. The reaction mixture underwent filtration through a short silica plug, and the filtrate was subjected to evaporation. The solid residue was subjected to purification through column chromatography, utilizing hexane as the eluent. This process yielded 3.67 grams (~99%) of pure product in the form of pale-yellow solid.

^{1}H NMR (400 MHz, $CDCl_3$) δ 7.51 (s, 3H), 0.25 (s, 27H).

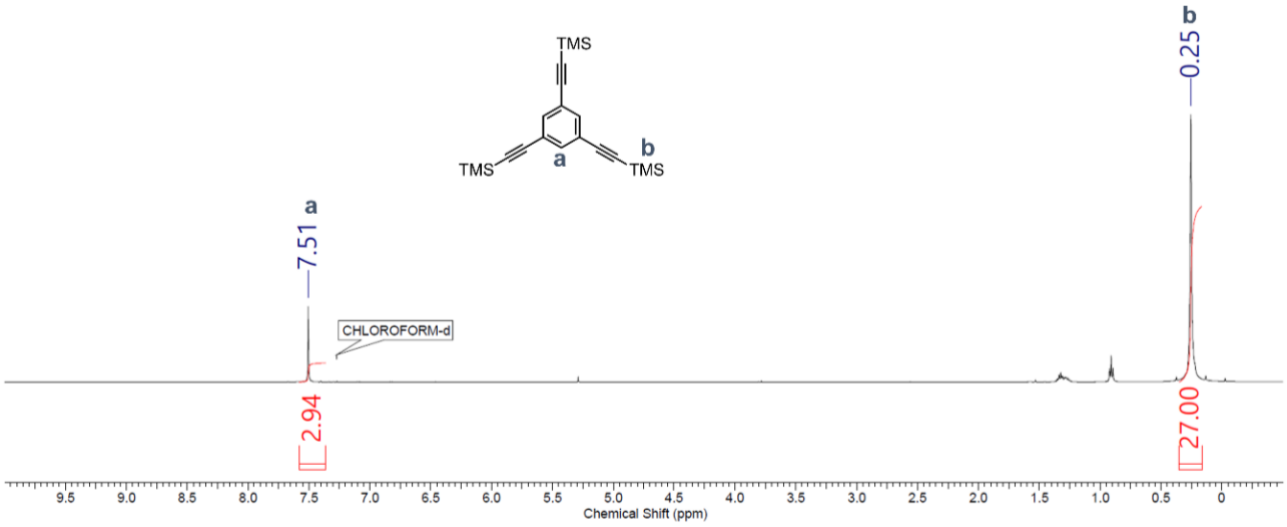

1,3,5-triethynylbenzene **(9)**[8, 19-21]:

In a 250 mL round-bottom flask, 3.67 grams (0.01 moles, 1 equivalent) of 1,3,5-tris((trimethylsilyl)ethynyl)benzene **(8)** was dissolved in a mixture of 90 mL of THF and 90 mL of MeOH. To this solution, 31 mL (0.031 moles, 3.1 eq.) of a 1.0M aqueous KOH solution was added dropwise, and the reaction mixture was stirred for 3 hours. The reaction was then halted, and 500 mL of $CHCl_3$ was introduced. The resulting mixture was transferred to an extraction funnel and washed successively with 500 mL of DI water and 500 mL of brine. The organic layers were subsequently dried over Na_2SO_4, and the solvent was evaporated under reduced pressure, yielding 1.45 grams (96.6%) of pure product in the form of a yellow solid.

^{1}H NMR (400 MHz $CDCl_3$): δ 7.58 (s, 3H), 3.11 (s, 3H).

^{13}C NMR (100 MHz; $CDCl_3$): δ 135.88, 123.19, 81.85, 78.91.

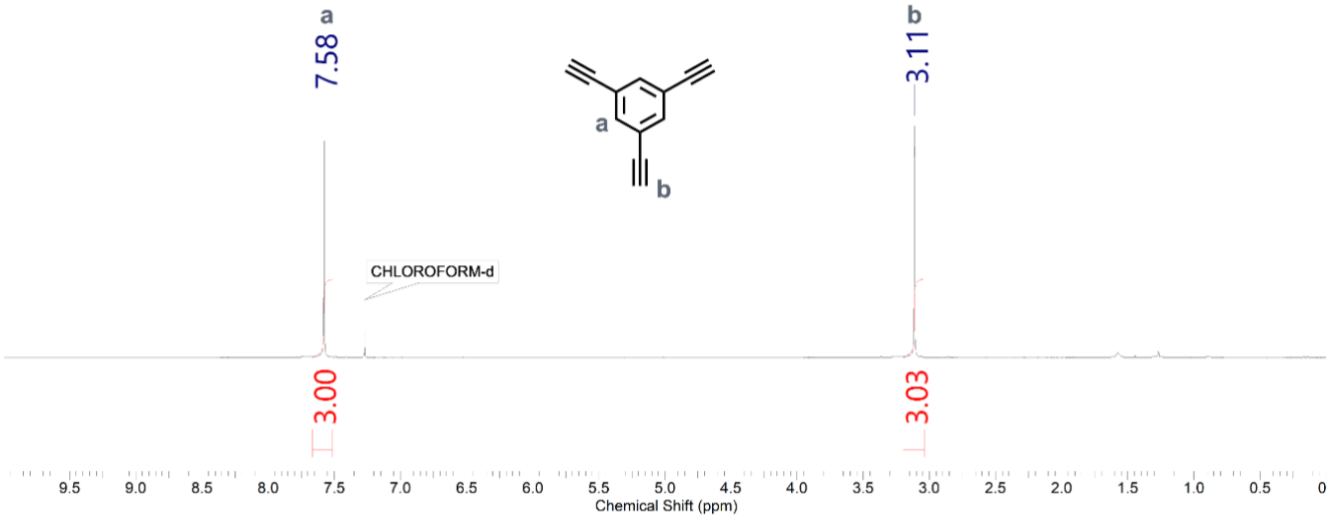

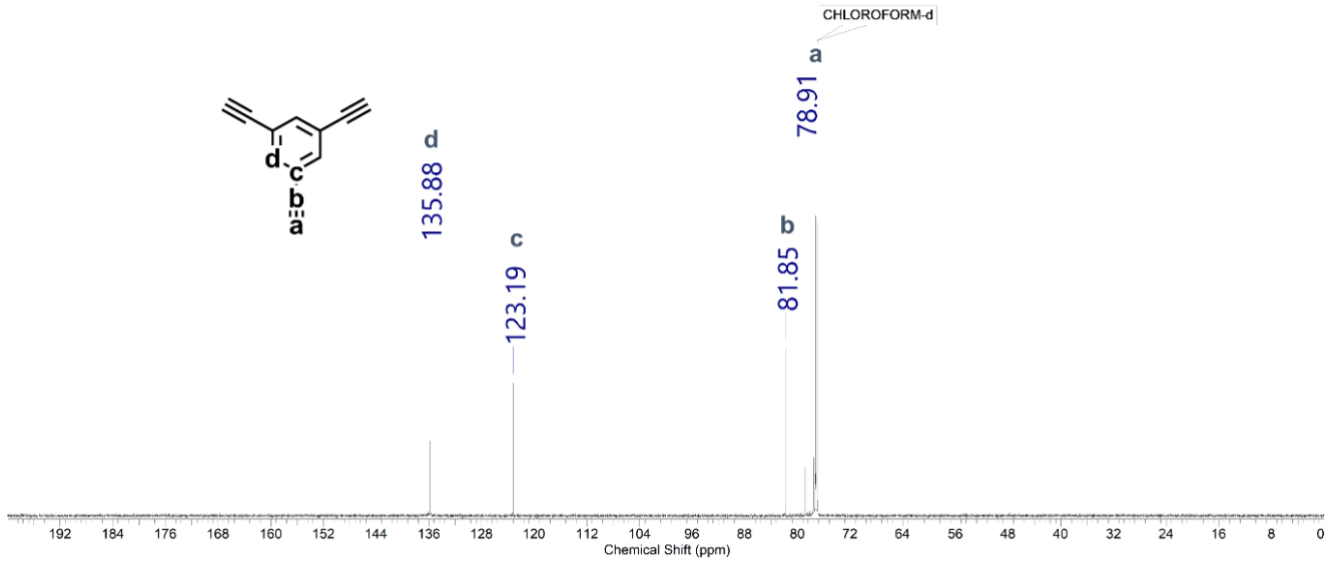

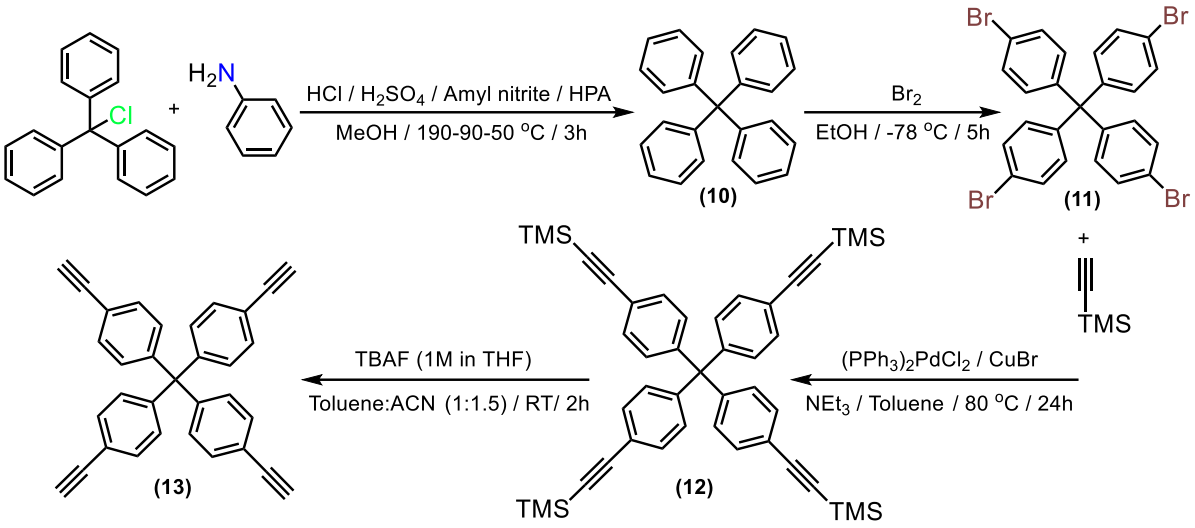

Tetraphenylmethane **(10)**[22-24]:

In a 500 mL three-neck round-bottom flask, flushed with argon and equipped with a mechanical stirrer, reflux condenser, and dropping funnel, 30.0 grams (107.6 mmol, 1 equivalent) of chlorotriphenylmethane and 19.65 mL (215.2 mmol, 2 equivalents) of freshly distilled aniline were combined. The mixture was heated to 190 °C for 15 minutes, during which a solid precipitated. This solid was isolated, ground into a powder, and subsequently placed in a 500 mL two-neck round-bottom flask along with 180 mL of methanol and 118 mL of 2M HCl. The mixture was heated at 90 °C for 1 hour, cooled to room temperature, filtered to collect the powder, and then dried under vacuum at 90 °C overnight.

In a 1L three-neck round-bottom flask, also flushed with argon and equipped with a mechanical stirrer, reflux condenser, and dropping funnel, the obtained off-white powder and 300 mL of DMF were combined. The reaction was cooled to -10 °C using a salt-ice bath, and then 34.41 mL (645.6 mmol, 6 equivalents) of sulfuric acid were added over the course of 1 hour. The dropping funnel was replaced under an argon flow, and 23.0 mL (177.56 mmol, 1.65 equivalents) of isopentyl nitrite were added at -10 °C over 30 minutes. The reaction mixture was stirred for 1 hour, after which a bubbler was attached to the flask, and 87.3 mL (1.61 mol, 15 equivalents) of hydrophosphorous acid (HPA) were added slowly. Hydrogen evolution was observed during this addition. After completing the addition, the suspension was heated to 50 °C until hydrogen evolution ceased. The mixture was then cooled to room temperature, filtered, and washed with DMF, water, and ethanol to yield 30.1 grams (87.3%) of pure product as an off-white powder.

^{1}H NMR (400 MHz $CDCl_3$): δ 7.09-7.19 (m, 20H).

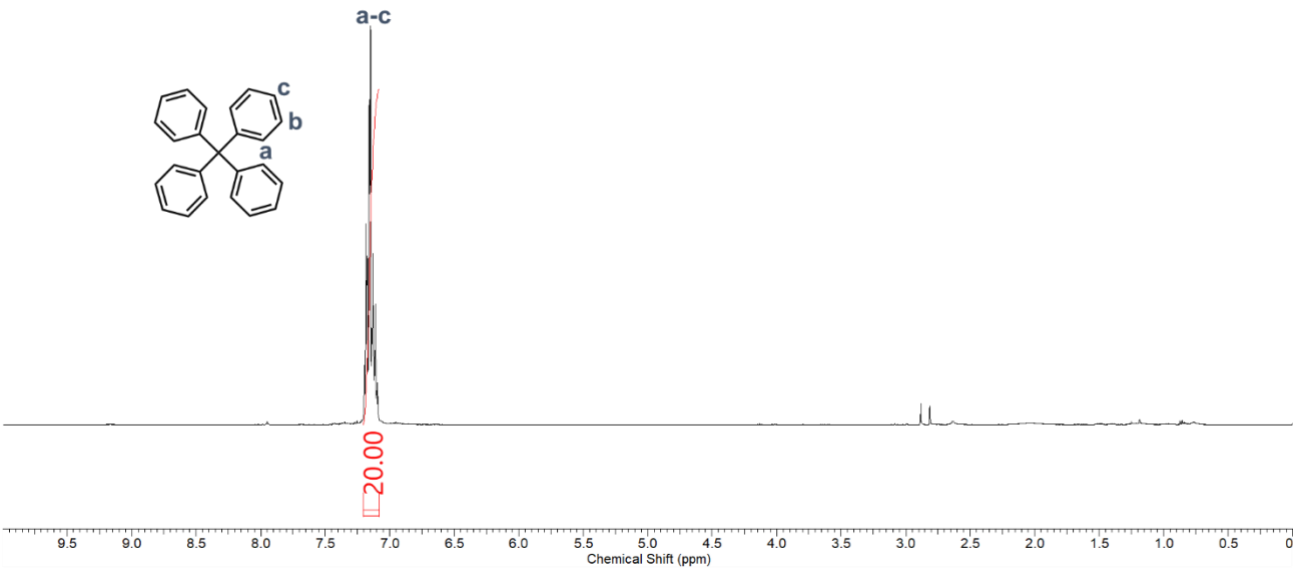

Tetrakis(4-bromophenyl)methane **(11)**[22-24]:

In a 100 mL three-necked round-bottom flask, 5.0 grams (15.6 mmol, 1 equivalent) of tetraphenylmethane **(10)** were placed, and then 16.0 mL (0.312 mol, 20 equivalents) of bromine were added dropwise with vigorous stirring at room temperature. After the addition was complete, the reaction mixture was stirred for an additional 20 minutes and then cooled to -78 °C, where 35 mL of ethanol was added slowly. Subsequently, the reaction mixture was allowed to warm to room temperature overnight. The resulting precipitate was filtered, washed with 25 mL of saturated aqueous $NaHSO_3$ solution and 25 mL of deionized water. The solid residue was dissolved in CH_2Cl_2, filtered twice, and the filtrate was evaporated under reduced pressure to yield 9.0 grams (90.7%) of pure product as a yellowish solid.

^{1}H NMR (400 MHz, DMSO-*d6*): δ 7.52 (d, *J*=8.7 Hz, 8H) 7.06 (d, *J*=8.8 Hz, 16H)

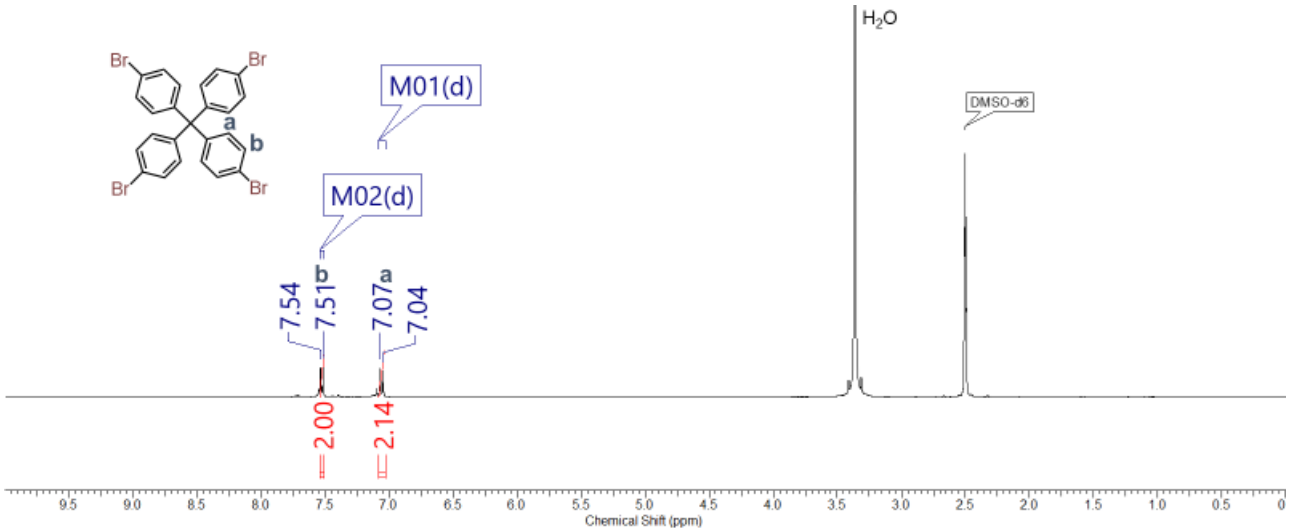

Tetrakis(4-ethynylphenyl)methane **(13)**[22-24]:

In a 500 mL Ar-flushed round-bottom flask, 3.0 grams (4.72 mmol, 1 equivalent) of tetrakis(4-bromophenyl)methane **(11)**, 186 mg (0.189 mmol, 0.04 equivalent) of bis(triphenylphosphine)palladium(II) chloride, and 27 mg (0.189 mmol, 0.04 equivalent) of copper(I) bromide were dissolved in 25 mL of anhydrous toluene and 36 mL of triethylamine under an inert atmosphere. Then, 4.0 mL (28.32 mmol, 6.0 equivalents) of trimethylsilylacetylene were added dropwise to the reaction mixture, and the resulting mixture was heated at 80 °C for 24 hours. After cooling to room temperature, the solvents were removed under reduced pressure. The solid residue was dissolved in 300 mL of diethyl ether and 120 mL of 1M aqueous HCl solution. The organic layers were separated, washed with 120 mL of deionized water, dried over $MgSO_4$, and the solvent was evaporated under reduced pressure. The product was used further without any additional purification or characterization.

In a 250 mL Ar-flushed round-bottom flask, 3.2 grams (4.50 mmol, 1 equivalent) of tetrakis(4-trimethylsilylethynyl)phenylmethane **(12)** was dissolved in a mixture of 60 mL of anhydrous toluene and 90 mL of anhydrous acetonitrile at room temperature. Then, 27 mL (27 mmol, 6.0 equivalents) of 1M tetrabutylammonium fluoride in THF was added dropwise and stirred at room temperature for 2 hours. Afterwards, the reaction mixture was poured into 150 mL of deionized water. The organic layers were separated, and the aqueous phase was extracted with CH_2Cl_2 (2 × 300 mL). The combined organic layers were dried over $MgSO_4$. The solvents were removed under reduced pressure, and the crude product was purified by column chromatography using a 1:1 hexane/toluene (v:v) mixture, yielding 1.5 grams (81.1%) of pure product as a yellow solid.

^{1}H NMR (400 MHz, $CDCl_3$): δ 7.40 (d, *J*=8.6 Hz, 8H) 7.13 (d, *J*=8.7 Hz, 8H).

^{13}C NMR (100 MHz, $CDCl_3$) δ: 146.20, 131.65, 130.74, 120.30, 83.17, 77.61, 64.80.

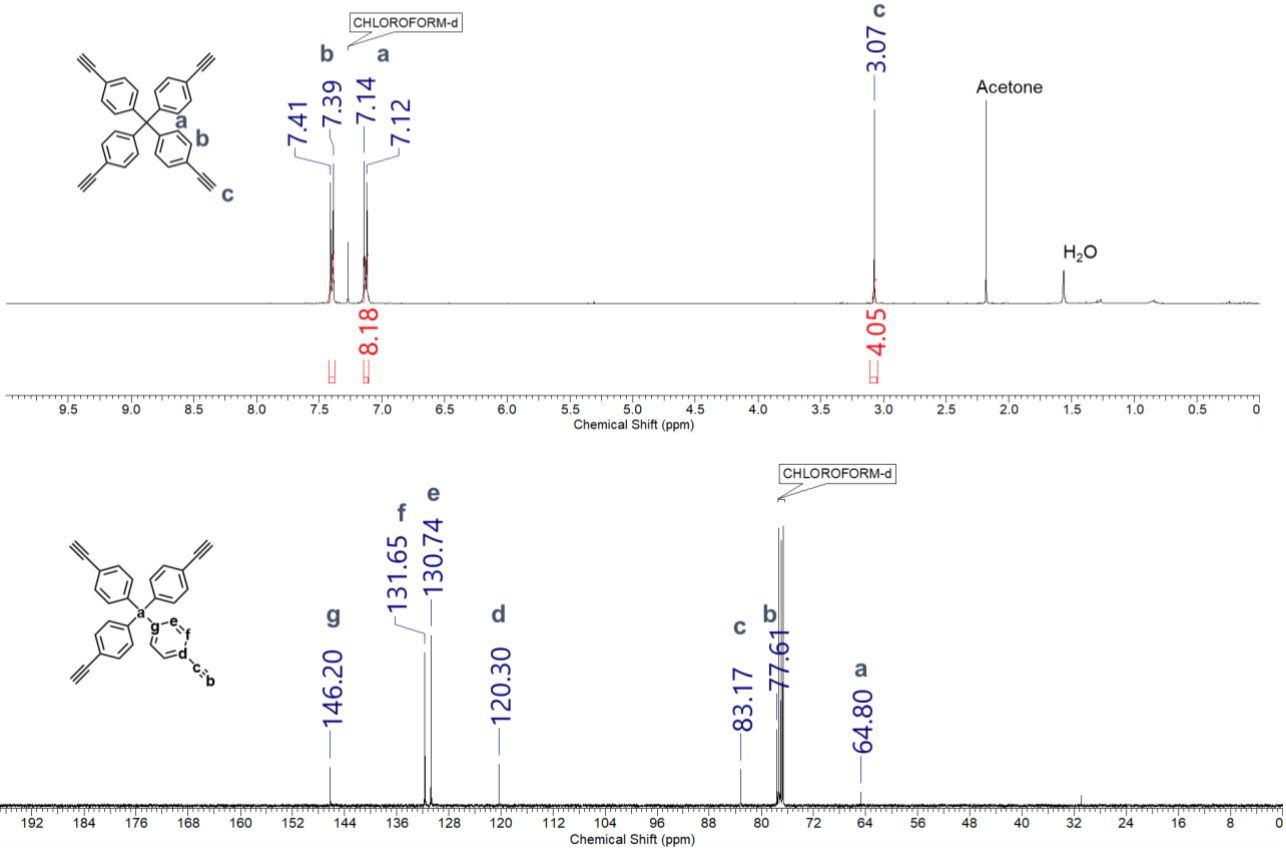

Experimental Procedures for Synthesis of the polymers:

Synthesis of porous polyphenylenes: Porous polyphenylenes were synthesized using previously described methods.[15, 17, 18]

2D-pPPs: In a Pyrex ampule, 26.6 milligrams (0.100 mmol, 3.0 equivalents) of 5,5'-(1,4-phenylene)bis(2H-pyran-2-one) and 10.0 milligrams (0.0667 mmol, 2.0 equivalents) of 1,3,5-triethynylbenzene were dissolved in 3 mL of 1,2,4-trichlorobenzene. The ampule contents were then sonicated for 10 minutes, subjected to three freeze-thaw cycles using liquid nitrogen for degassing, and flame sealed. The sealed ampule was placed in an oven and heated at 300 °C (ramping at 10 K/min) for 72 hours. After cooling to room temperature, the ampule was opened, and the contents were transferred into 200 mL of THF. Solids were isolated by filtration and subsequently washed with 200 mL of hexane, methanol, deionized water, and acetone. The polymer was further purified using Soxhlet extraction with methanol for 4 days to yield 27.1 mg (97.4%) of 2D-pPPs and finally dried under vacuum at 90 °C before characterization.

3D-pPPs: Similarly, in a Pyrex ampule, 26.6 milligrams (0.100 mmol, 2.0 equivalents) of 5,5'-(1,4-phenylene)bis(2H-pyran-2-one) and 20.8 milligrams (0.050 mmol, 1.0 equivalent) of 1,3,5-triethynylbenzene were dissolved in 3 mL of 1,2,4-trichlorobenzene. The ampule contents underwent sonication for 10 minutes, followed by degassing through three freeze-thaw cycles using liquid nitrogen, and subsequent flame sealing. The sealed ampule was heated in an oven at 300 °C (ramping at 10 K/min) for 72 hours. After cooling to room temperature, the ampule was opened, and the contents were transferred into 200 mL of THF. Solids were isolated by filtration and washed with 200 mL of hexane, methanol, deionized water, and acetone. The polymer underwent purification using Soxhlet extraction with methanol for 4 days to yield 36.9 mg (95.6%) of 3D-pPPs and was eventually dried under vacuum at 90 °C before characterization.

Structural characterization of the polymers

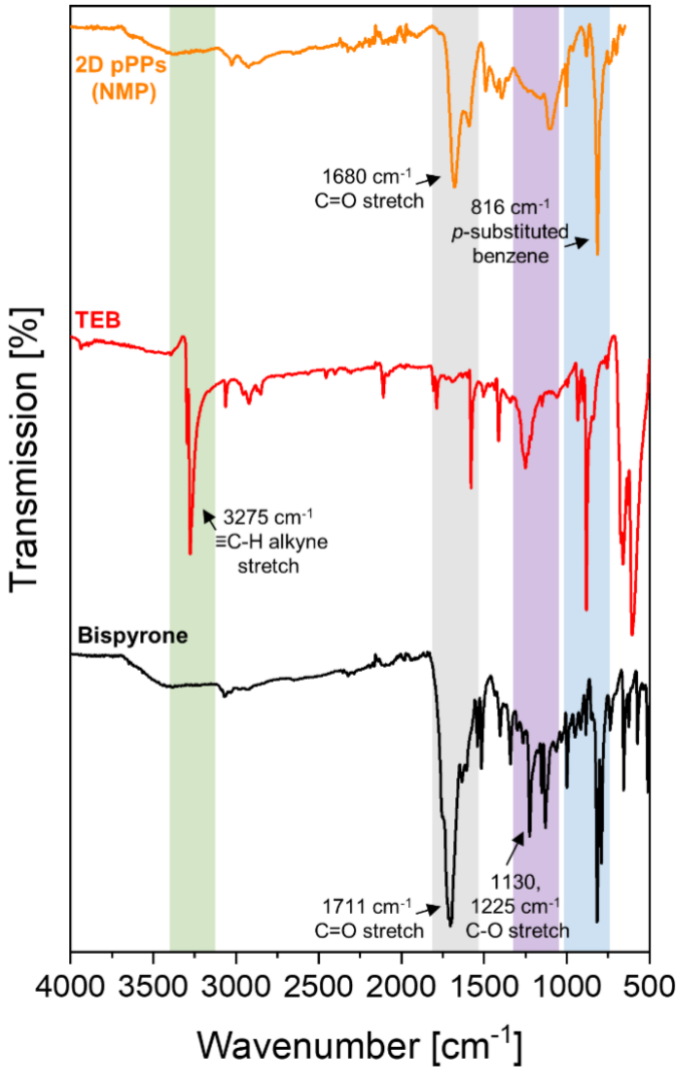

Figure S1. FTIR spectra of 2D-pPPs prepared in NMP. As it can be seen here, unreacted -C=O vibrations can be seen at 1680 cm^{-1}.

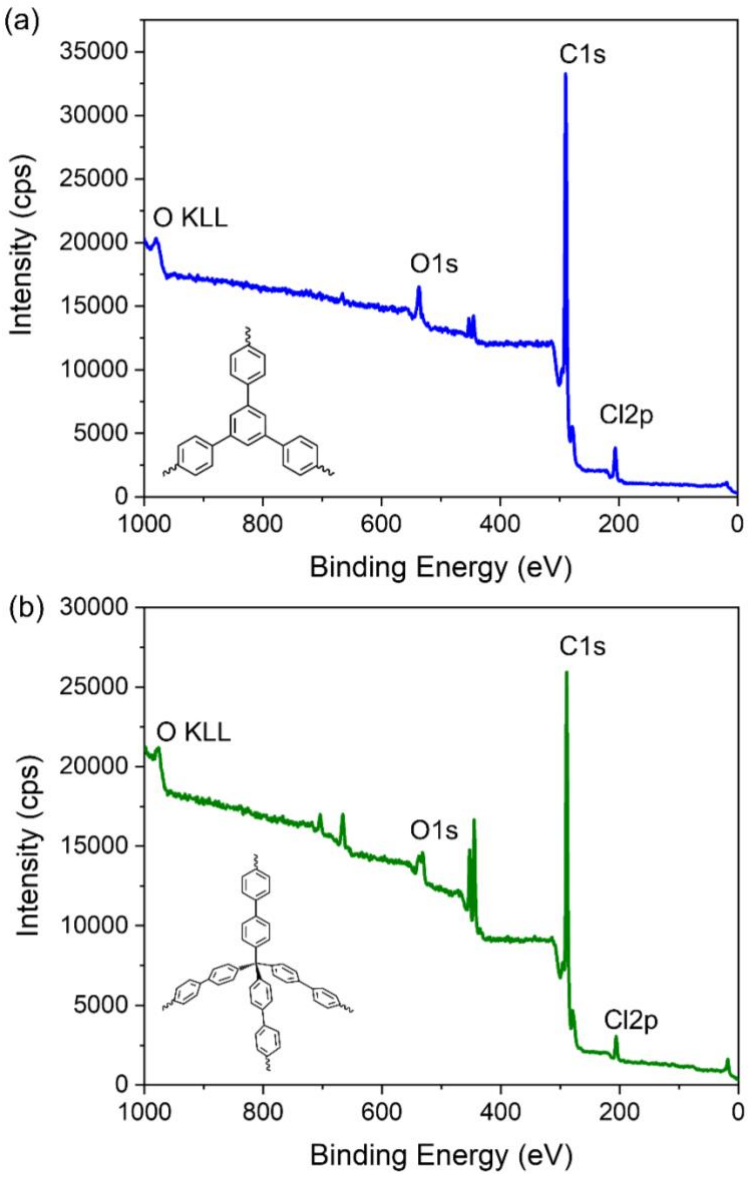

Figure S2. XPS survey spectra of a) 2D-pPPs and b) 3D-pPPs.

Table S1. The C1s binding energy and surface concentration from the XPS spectra of 2D-pPPs.

Sample	Method	C (%)	H (%)	O (%)	Cl (%)
2D-pPPs	XPS	92.55	-	4.70	2.74
	EA	90.68	4.07	5.25[a]	-
	Calculated	94.25	5.75	-	-
3D-pPPs	XPS	90.45	-	6.95	2.61
	EA	88.41	5.00	6.59[a]	-
	Calculated	94.29	5.71	-	-

[a] Oxygen amount is calculated by subtracting the amount of carbon and hydrogen from the total. While the oxygen amount is primarily attributed to the presence of C=O end groups, the presence of moisture, residual solvents and gases can also contribute to the oxygen content.

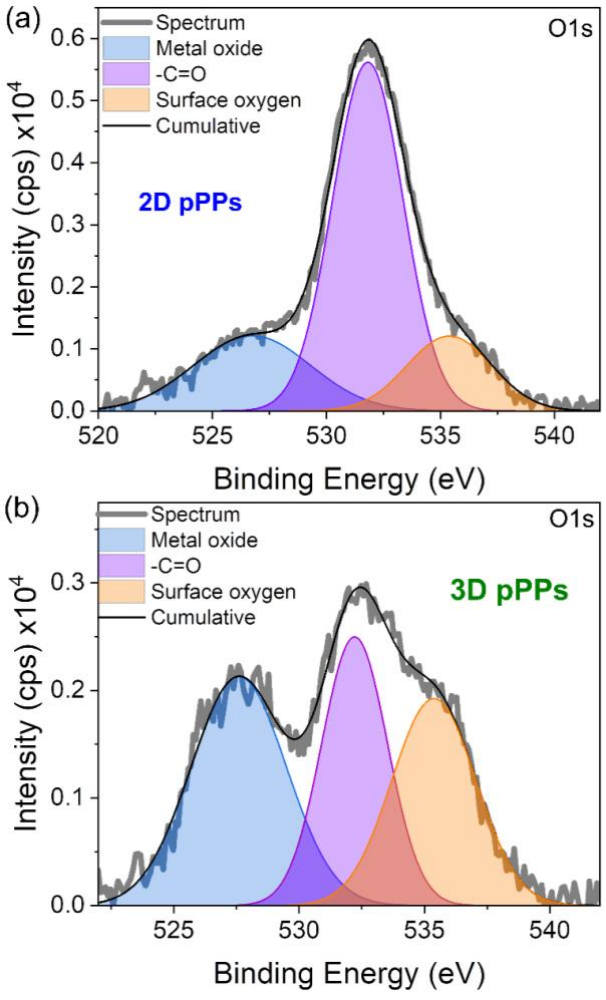

Figure S3. High-resolution XPS O1s spectra of 2D-pPPs and 3D-pPPs.

Table S2. The C1s binding energy and surface concentration from the XPS spectra of 2D-pPPs.

2D-pPPs			3D-pPPs		
Binding energy (eV)	Chemical bonds	Concentration (%)	Binding energy (eV)	Chemical bonds	Concentration (%)
-	-	-	282.7	sp^3 carbon	3.8
285.0	sp^2 carbon	89.6	285.0	sp^2 carbon	84.3
290.9	π- π*	10.4	291.2	π- π*	11.9

Table S3. The O1s binding energy and surface concentration from the XPS spectra of 2D-pPPs.

2D-pPPs			3D-pPPs		
Binding energy (eV)	Chemical bonds	Concentration (%)	Binding energy (eV)	Chemical bonds	Concentration (%)
526.7	Metal oxide	22.1	527.6	Metal oxide	38.4
531.8	-C=O	61.9	532.2	-C=O	31.0
535.4	Surface oxygen	16.0	535.4	Surface oxygen	30.6

Table S4. BET surface areas and pore volumes of 2D and 3D-pPPs obtained from N_2 uptake isotherms at 77K.

Sample	BET[a] [$m^2\ g^{-1}$]	S_{micro}[b] [$m^2\ g^{-1}$]	S_{ext}[c] [$m^2\ g^{-1}$]	V_{total}[d] [$cm^3\ g^{-1}$]	V_{micro}[e] [$cm^3\ g^{-1}$]	V_{ext}[f] [$cm^3\ g^{-1}$]
2D-pPPs	1553	618	934	1.45	0.26	1.19
3D-pPPs	1536	569	967	1.27	0.24	1.03

[a] BET surface area calculated over the pressure range (P/P_0) of 0.01–0.18 (Fig. S8). [b] Micropore surface area calculated using the *t*-plot method. [c] $S_{ext} = S_{total} - S_{micro}$. [d] Total pore volume obtained at P/P_0=0.95. [e] Micropore volume calculated using *t*-plot method. [f] $V_{ext} = V_{total} - V_{micro}$.

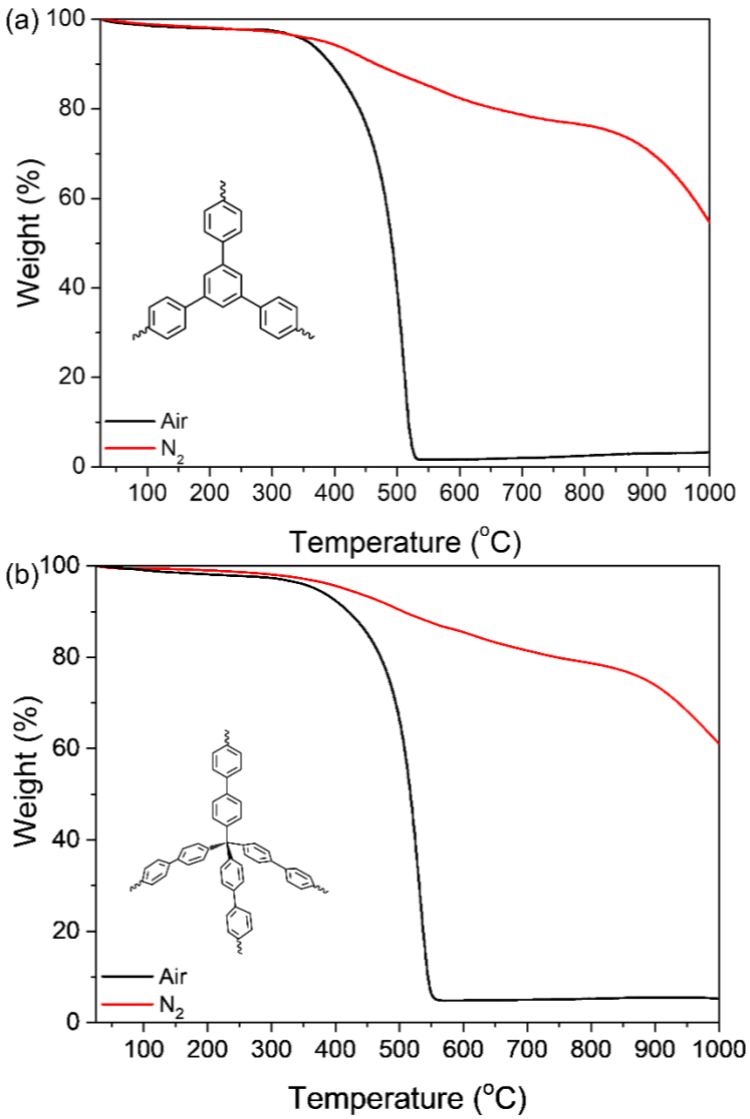

Figure S4. Thermogravimetric analysis (TGA) curves of a) 2D-pPPs and b) 3D-pPPs under air (black) and N_2 (black) flow.

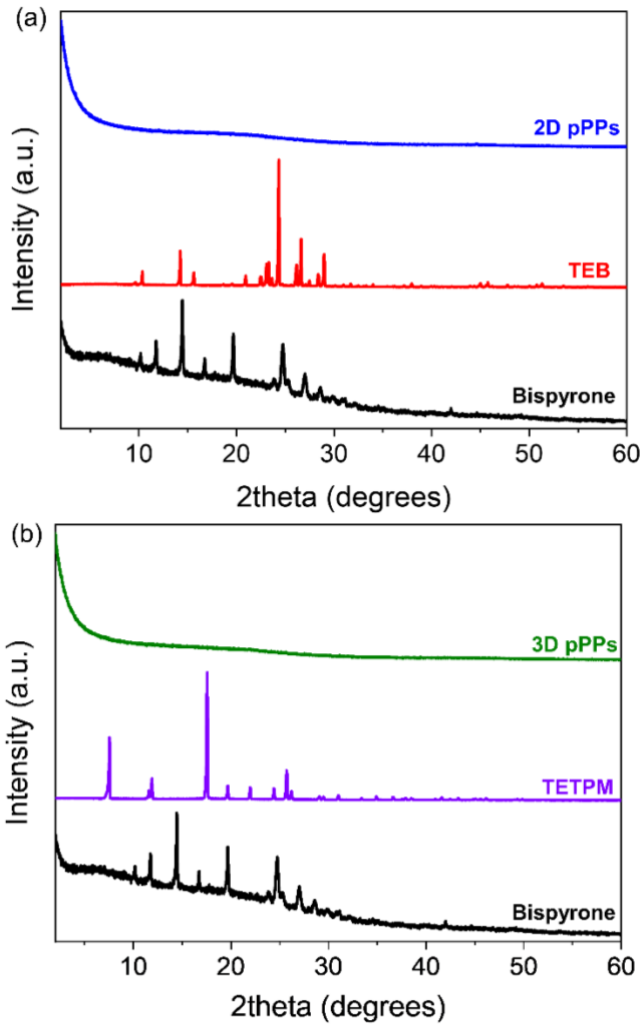

Figure S5. XRD diffractograms of a) 2D-pPPs and b) 3D-pPPs.

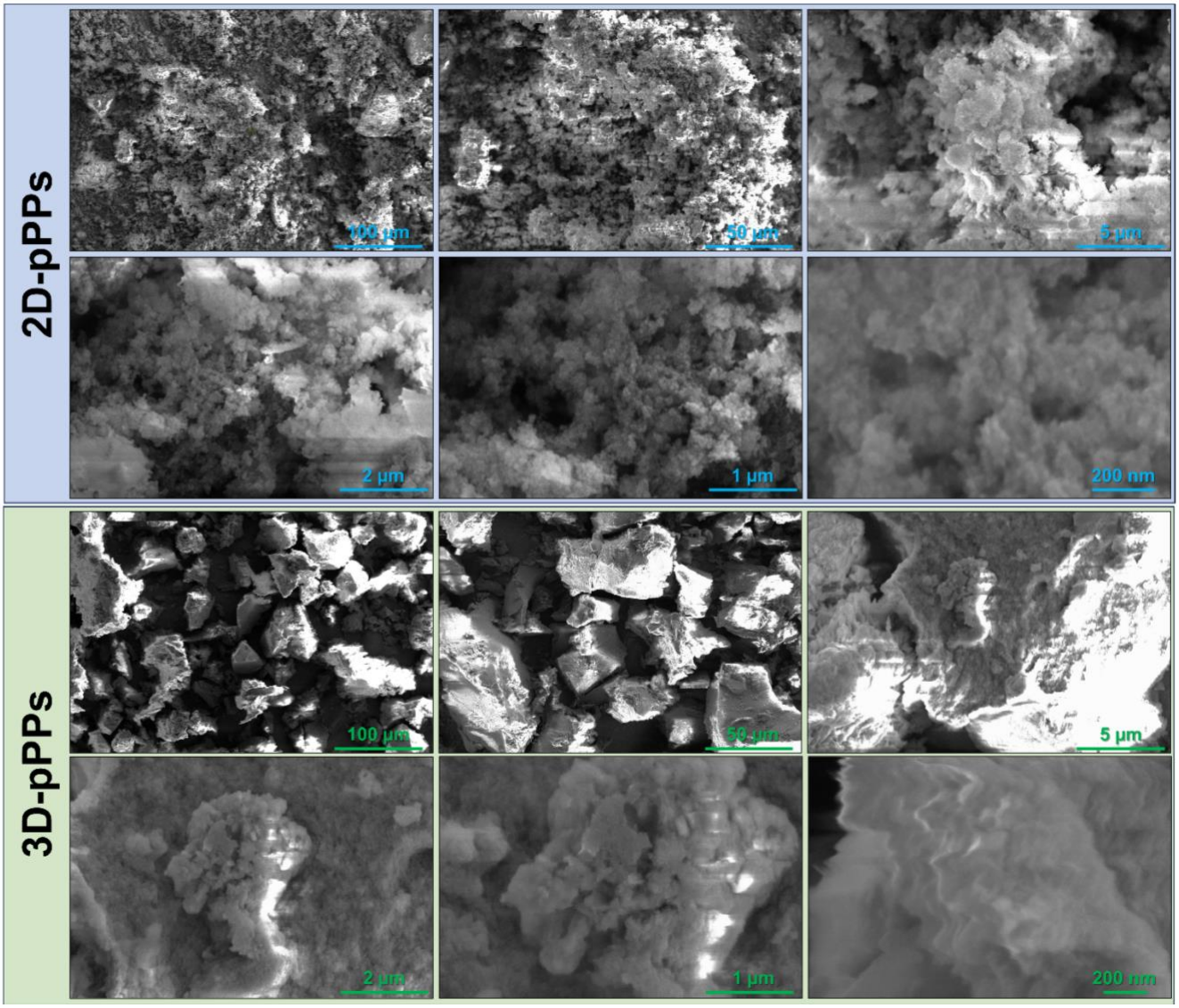

Figure S6. SEM micrographs of 2D-pPPs (top) and 3D-pPPs (bottom).

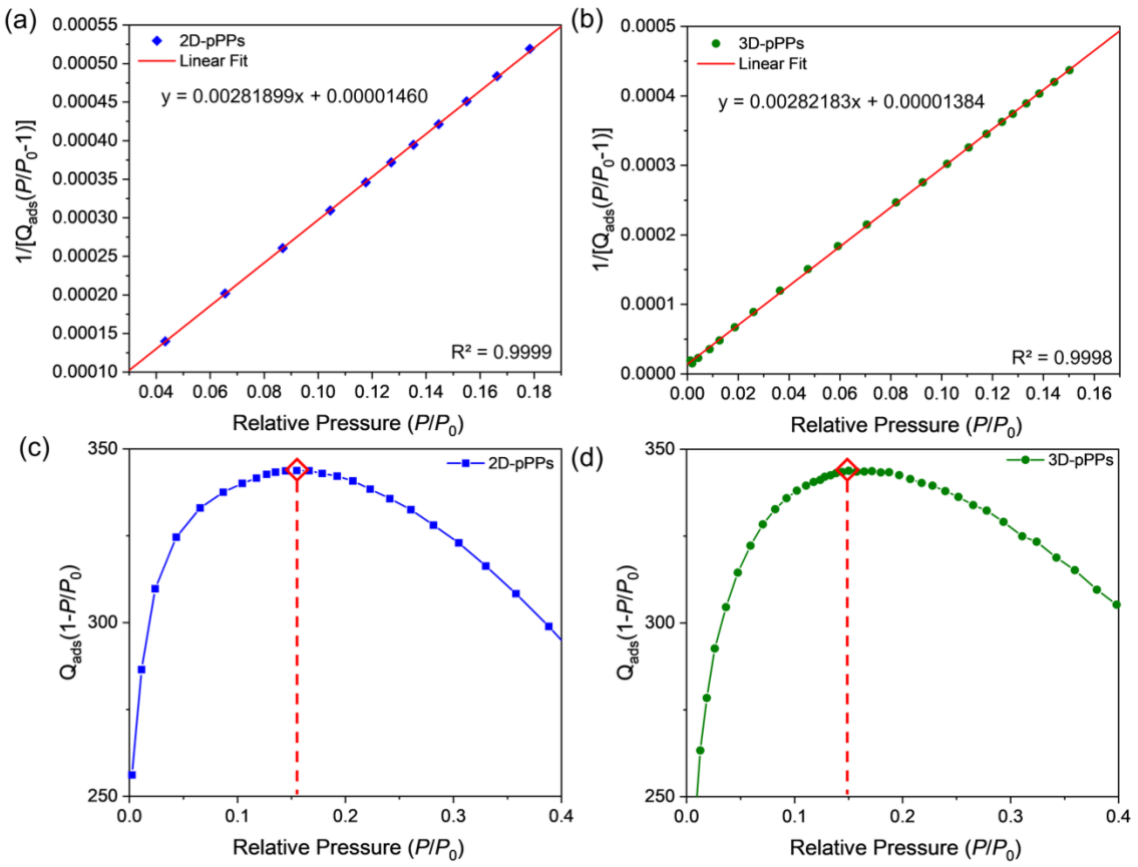

Figure S7. BET plots with fits of a) 2D-pPPs and b) 3D-pPPs obtained from N_2 adsorption isotherms at 77K. Enlarged calculated Rouquerol plots for c) 2D-pPPs and d) 3D-pPPs. Red pointer shows the P/P_0 at maximum $Q_{ads}[1-P/P_0]$ term.

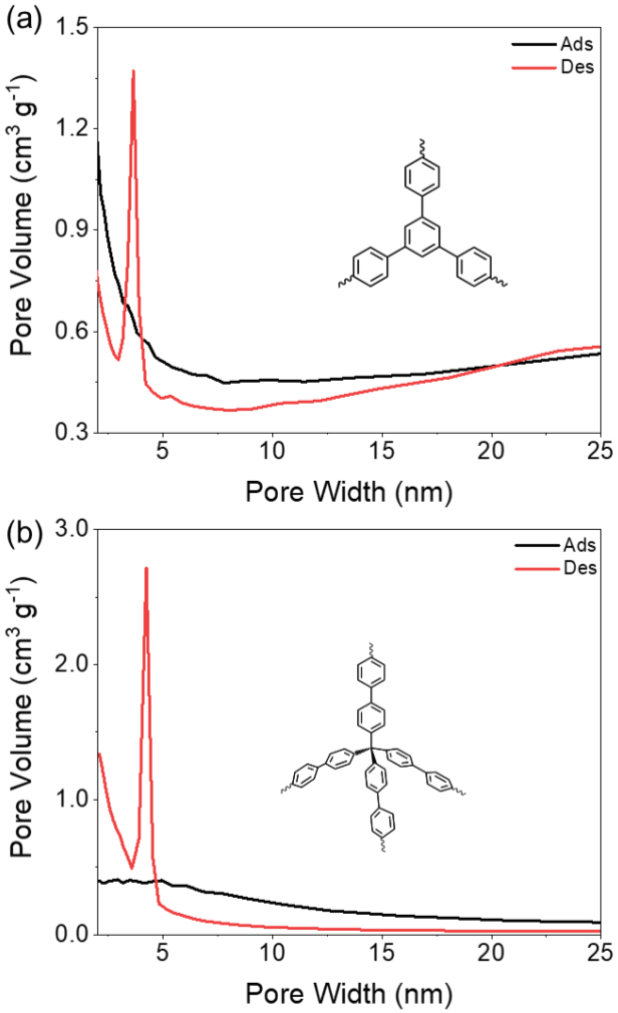

Figure S8. BJH pore size distribution plots of a) 2D-pPPs and b) 3D-pPPs. Ads represent pore size analysis derived from adsorption isotherms and Des from desorption isotherms, respectively.

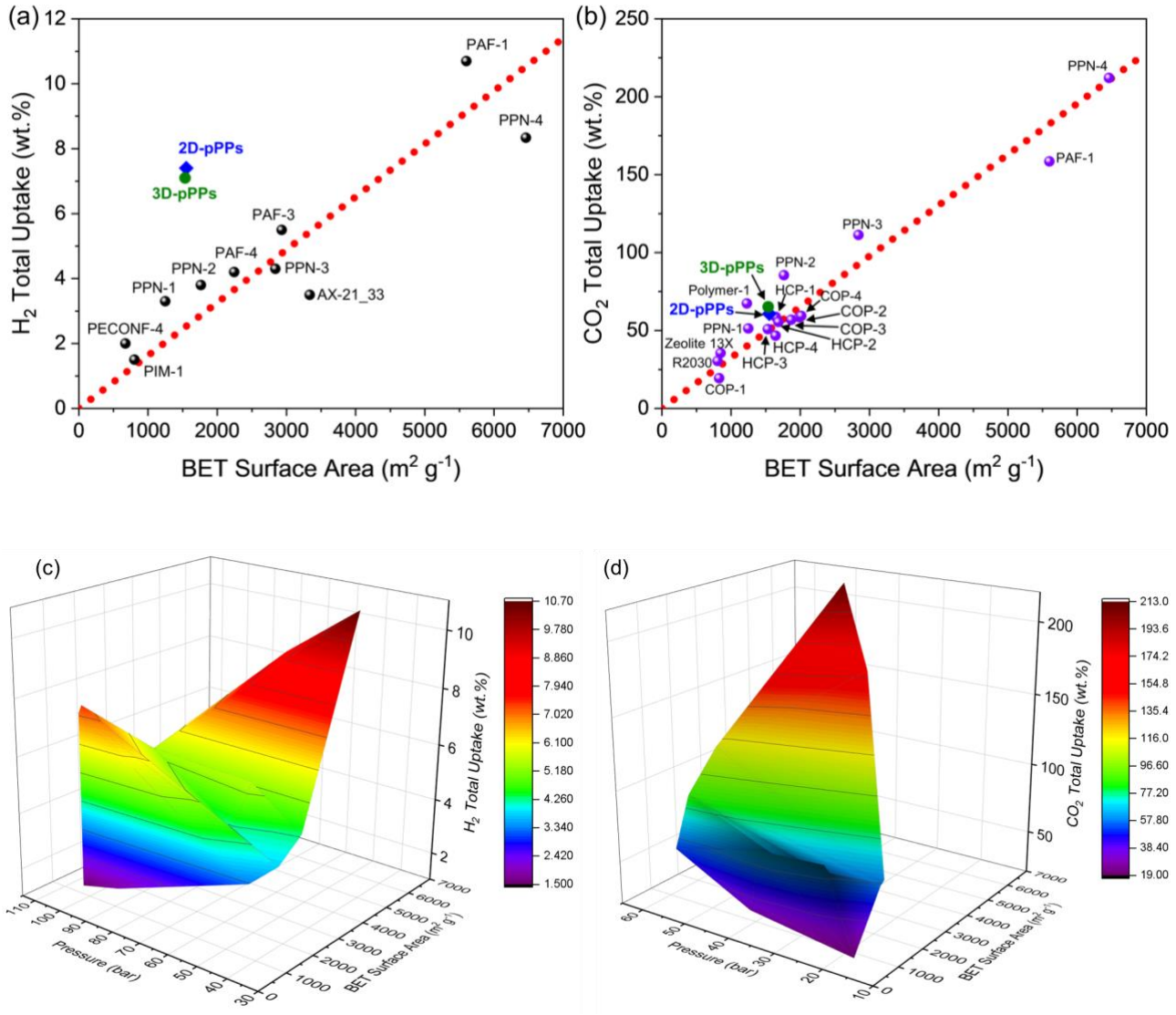

Figure S9. Comparison of 2D and 3D-pPPs with other reported porous organic polymers in terms of a-c) H_2 and b-d) CO_2 uptake.

Table S5. The H_2 uptake performance of 2D and 3D-pPPs in comparison with reported literature.

Polymer	BET Surface Area [$m^2\ g^{-1}$]	Pore Size [nm]	H_2 uptake [wt.%] at 77K	Q_{st} [kJ mol^{-1}][a]	Reference
PAF-3	2932	1.3	5.5 at 60 bars	6.6[b]	[25]
PAF-4	2246	1.2	4.2 at 60 bars	6.3[b]	
PPN-1	1249	0.6	3.3 at 45 bars	7.6	[22]
PPN-2	1764	1.2	3.8 at 40 bars	6.9	
PPN-3	2840	1.2	4.3 at 42 bars	5.5	
PPN4	6461	1.2	8.34 at 80 bars	4.0	[26]
PAF-1	5600	1.4	10.7 at 48 bars	4.6	[27]
PIM-1	804.0	0.9	1.5 at 100 bars	-	[28]
AX-21_33	3336	-	3.5 at 100 bars	5.2	[29]
PECONF-4	673	0.45	2.0 at 85 bars	10.5	[30]
2D-pPPs	1553	1.2	7.4 at 108 bars	5.4	This work
3D-pPPs	1536	1.2	7.1 at 109 bars	5.1	

[a] Q_{st} is reported at zero coverage. [b] Q_{st} values are derived from low pressure adsorption isotherms.

Table S6. The CO_2 uptake performance of 2D and 3D-pPPs in comparison with reported literature.

Polymer	BET Surface Area [$m^2\ g^{-1}$]	Pore Size [nm]	CO_2 uptake [wt.%] at 296K	Q_{st} [kJ mol^{-1}][a]	Reference
PPN-1	1249	0.6	51.3[b] at 60 bars	~27.5	22
PPN-2	1764	1.2	85.5[b] at 60 bars	~22.5	
PPN-3	2840	1.2	111.3 at 60 bars	~18.6	
PPN4	6461	1.2	212.1 at 50 bars	-	26
PAF-1	5600	1.4	158.5 at 40 bars	-	27
HCP-1	1646	1.2	58.7 at 30 bars	23.5	31
HCP-2	1684	1.1	55.5 at 30 bars	21.2	
HCP-3	1531	1.2	50.9 at 30 bars	22.1	
HCP4	1642	1.0	46.7 at 30 bars	21.6	
Polymer 1	1228	-	67.4 at 40 bars	30	32
R2030	806	-	30.4 at 40 bars	-	
Zeolite 13X	848	-	35.5 at 40 bars	-	
COP-1	827	0.5	19.4 at 18 bars	-	33
COP-2	1986	0.6	58.5 at 18 bars	-	
COP-3	1869	0.4	56.9 at 18 bars	-	
COP-4	2015	0.4	59.4 at 18 bars	-	
2D-pPPs	1553	1.2	60.7 at 27 bars	25.1	This work
3D-pPPs	1536	1.2	65.2 at 28 bars	24.1	

[a] Q_{st} is reported at zero coverage. [b] Uptake values are estimated from the graphs.

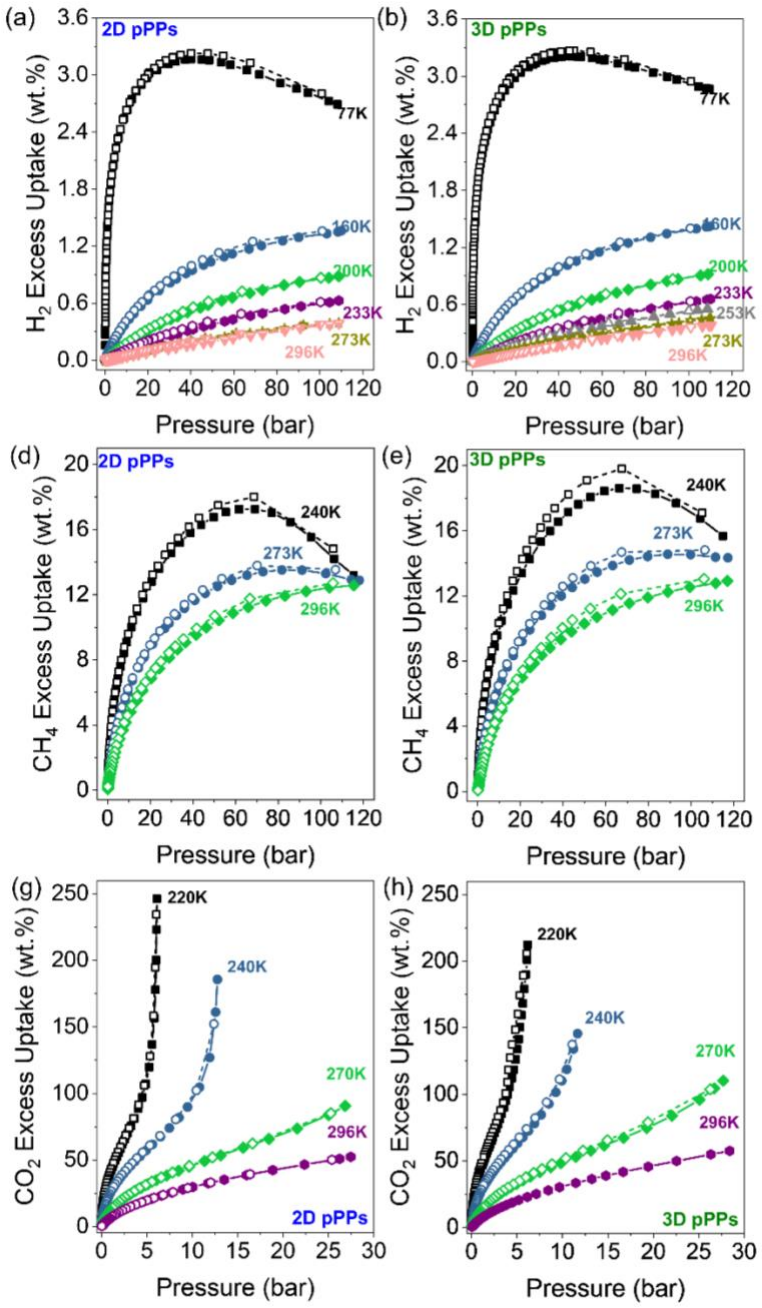

Figure S10. H_2 excess uptake isotherms of a) 2D-pPPs and b) 3D-pPPs. CH_4 excess uptake isotherms of c) 2D-pPPs and d) 3D-pPPs. CO_2 excess uptake isotherms of e) 2D-pPPs and f) 3D-pPPs. Filled and empty symbols represent adsorption and desorption branches respectively.

Table S7. The H_2, CO_2 and CH_4 uptake performance of 2D and 3D-pPPs in comparison with reported literature.

	H_2 uptake [wt.%]				CH_4 uptake [wt.%]				CO_2 uptake [wt.%]			
T (K)	Total		Excess		Total		Excess		Total		Excess	
	2D-pPPs	3D-pPPs	2D-pPPs	3D-pPPs	2D-pPPs	3D-pPPs	2D-pPPs	3D-pPPs	2D-pPPs	3D-pPPs	2D-pPPs	3D-pPPs
77	7.4	7.1	2.7	2.9	-	-	-	-	-	-	-	-
160	3.5	3.3	1.4	1.4	-	-	-	-	-	-	-	-
200	2.6	2.5	1.1	1.1	-	-	-	-	-	-	-	-
220	-	-	-	-	-	-	-	-	248.6	214.5	246.3	212.4
233	2.1	2.0	1.1	0.7	-	-	-	-	-	-	-	-
240	-	-	-	-	35.5	35.3	13.2	15.7	190.5	149.4	185.7	145.6
253	-	1.8	0.6	0.6	-	-	-	-	-	-	-	-
270	-	-	-	-	-	-	-	-	100.4	119.3	90.6	110.2
273	1.7	1.6	0.4	0.5	28.7	28.2	12.9	14.3	-	-	-	-
296	1.6	1.5	0.4	0.4	25.6	24.6	12.6	12.9	60.7	65.2	52.4	57.5

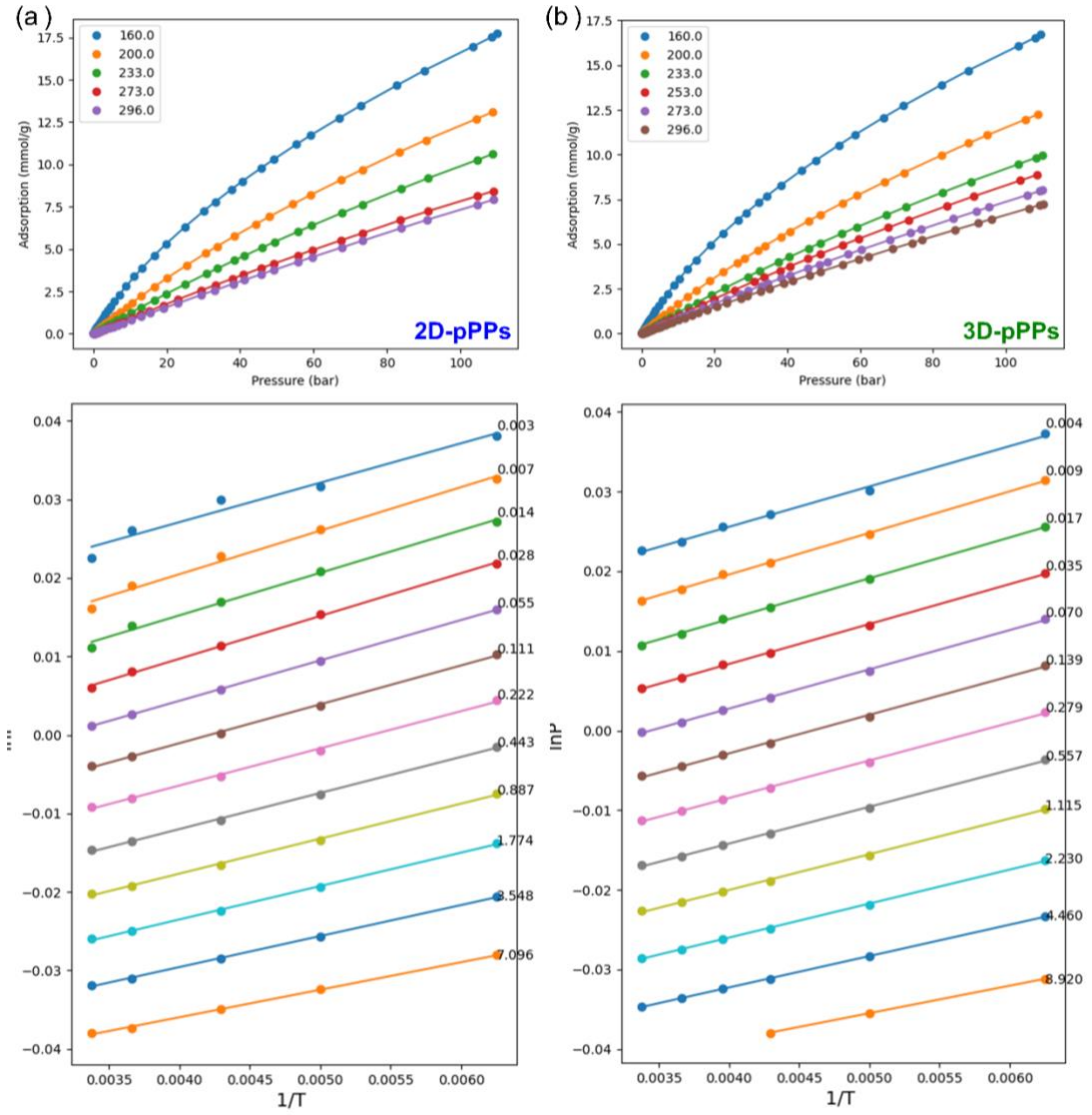

Figure S11. H_2 adsorption isotherm fits at different temperatures and lnP vs 1/T plots for a) 2D-pPPs and b) 3D-pPPs.

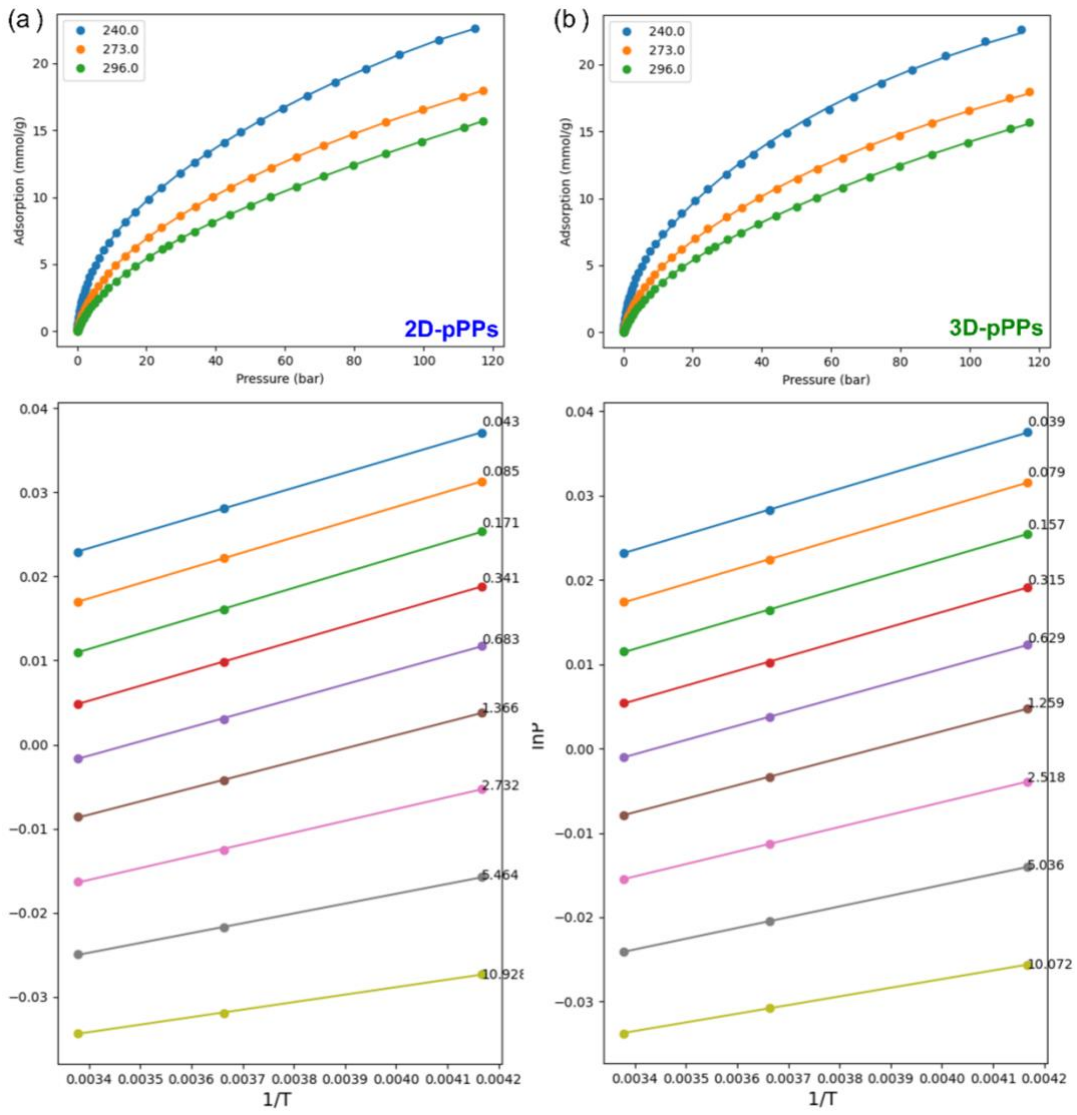

Figure S12. CH_4 adsorption isotherm fits at different temperatures and lnP vs 1/T plots for a) 2D-pPPs and b) 3D-pPPs.

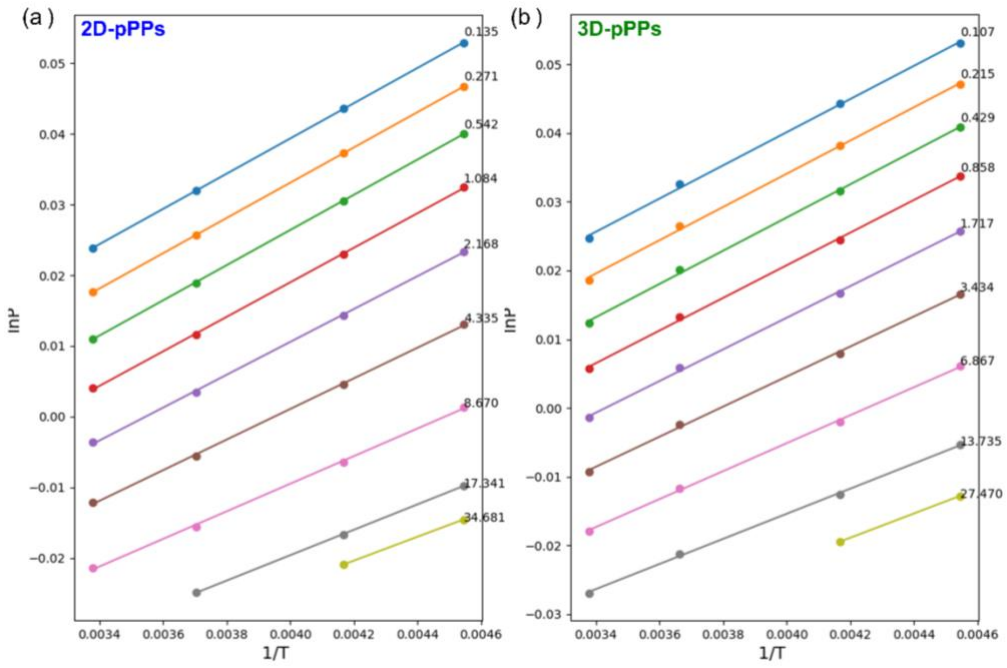

Figure S13. CO_2 adsorption isotherm fits at different temperatures and lnP vs 1/T plots for a) 2D-pPPs and b) 3D-pPPs.

References

1. M. Wojdyr, *J. Appl. Crystallogr.*, 2010, **43**, 1126-1128.

2. J. Jagiello, J. Kenvin, C. O. Ania, J. B. Parra, A. Celzard and V. Fierro, *Carbon*, 2020, **160**, 164-175.

3. W. Zhou, H. Wu, M. R. Hartman and T. Yildirim, *J. Phys. Chem. C*, 2007, **111**, 16131-16137.

4. Y. Peng, V. Krungleviciute, I. Eryazici, J. T. Hupp, O. K. Farha and T. Yildirim, *J. Am. Chem. Soc.*, 2013, **135**, 11887-11894.

5. K. Yoosaf, A. Llanes-Pallas, T. Marangoni, A. Belbakra, R. Marega, E. Botek, B. Champagne, D. Bonifazi and N. Armaroli, *Chem. Eur. J.*, 2011, **17**, 3262-3273.

6. C. Mechtler, M. Zirngast, W. Gaderbauer, A. Wallner, J. Baumgartner and C. Marschner, *J. Organomet. Chem.*, 2006, **691**, 150-158.

7. I. J. Olavarria-Contreras, M. L. Perrin, Z. Chen, S. Klyatskaya, M. Ruben and H. S. J. van der Zant, *J. Am. Chem. Soc.*, 2016, **138**, 8465-8469.

8. M. I. Mangione, R. A. Spanevello, A. Rumbero, D. Heredia, G. Marzari, L. Fernandez, L. Otero and F. Fungo, *Macromolecules*, 2013, **46**, 4754-4763.

9. A. V. S. Bogdanova, M. F., *Izv. Akad. Nauk, Ser. Khim.*, 1957, **2**, 224-229.

10. H. S. Vratislava Kvita, *Helv. Chim. Acta*, 1990, **73**, 883-889.

11. H. J. Minnemeyer, J. A. Egger, J. F. Holland and H. Tieckelmann, *J. Org. Chem.*, 1961, **26**, 4425-4429.

12. A. N. Nesmeyanov, Freydlina, R. H., Zakharkin, L. I., *Dokl. Akad. Nauk SSSR*, 1954, **XCVII**, 91-94.

13. D. S. Werner Schroth, Ulrich Jahn, Roland Spitzner, *Z. Chem., 29. Jg.*, 1989, **29**, 419-420.

14. L. I. Zakharkin and A. P. Pryanishnikov, *Bull. Acad. Sci. USSR, Div. Chem. Sci.*, 1983, **32**, 312-314.

15. J. K. Stille and Y. Gilliams, *Macromolecules*, 1971, **4**, 515-517.

16. E. T. Chukovskaya, A. A. Kamyshova and R. K. Freidlina, *Bull. Acad. Sci. USSR, Div. Chem. Sci.*, 1965, **14**, 445-449.

17. C. L. Schilling, Jr., J. A. Reed and J. K. Stille, *Macromolecules*, 1969, **2**, 85-88.

18. J. N. Braham, T. Hodgins, T. Katto, R. T. Kohl and J. K. Stille, *Macromolecules*, 1978, **11**, 343-346.

19. M. I. Mangione, R. A. Spanevello and M. B. Anzardi, *RSC Adv.*, 2017, **7**, 47681-47688.

20. R. W. Tilford, W. R. Gemmill, H.-C. zur Loye and J. J. Lavigne, *Chem. Mater.*, 2006, **18**, 5296-5301.

21. A. Schwartzen, L. Siebe, J. Schwabedissen, B. Neumann, H.-G. Stammler and N. W. Mitzel, *Eur. J. Inorg. Chem.*, 2018, **2018**, 2533-2540.

22. W. Lu, D. Yuan, D. Zhao, C. I. Schilling, O. Plietzsch, T. Muller, S. Bräse, J. Guenther, J. Blümel, R. Krishna, Z. Li and H.-C. Zhou, *Chem. Mater.*, 2010, **22**, 5964-5972.

23. K. Peschko, A. Schade, S. B. L. Vollrath, U. Schwarz, B. Luy, C. Muhle-Goll, P. Weis and S. Bräse, *Chem. Eur. J.*, 2014, **20**, 16273-16278.

24. X. Zhang, X. Zhang, J. A. Johnson, Y.-S. Chen and J. Zhang, *J. Am. Chem. Soc.*, 2016, **138**, 8380-8383.

25. T. Ben, C. Pei, D. Zhang, J. Xu, F. Deng, X. Jing and S. Qiu, *Energy Environ. Sci.*, 2011, **4**, 3991-3999.

26. D. Yuan, W. Lu, D. Zhao and H.-C. Zhou, *Adv. Mater.*, 2011, **23**, 3723-3725.

27. T. Ben, H. Ren, S. Ma, D. Cao, J. Lan, X. Jing, W. Wang, J. Xu, F. Deng, J. M. Simmons, S. Qiu and G. Zhu, *Angew. Chem. Int. Ed.*, 2009, **48**, 9457-9460.

28. K. Polak-Kraśna, R. Dawson, L. T. Holyfield, C. R. Bowen, A. D. Burrows and T. J. Mays, *J. Mater. Sci.*, 2017, **52**, 3862-3875.

29. M. Schlichtenmayer and M. Hirscher, *Appl. Phys. A*, 2016, **122**, 379.

30. M. Murialdo, N. J. Weadock, Y. Liu, C. C. Ahn, S. E. Baker, K. Landskron and B. Fultz, *ACS Omega*, 2019, **4**, 444-448.

31. C. F. Martín, E. Stöckel, R. Clowes, D. J. Adams, A. I. Cooper, J. J. Pis, F. Rubiera and C. Pevida, *J. Mater. Chem.*, 2011, **21**, 5475-5483.

32. R. T. Woodward, L. A. Stevens, R. Dawson, M. Vijayaraghavan, T. Hasell, I. P. Silverwood, A. V. Ewing, T. Ratvijitvech, J. D. Exley, S. Y. Chong, F. Blanc, D. J. Adams, S. G. Kazarian, C. E. Snape, T. C. Drage and A. I. Cooper, *J. Am. Chem. Soc.*, 2014, **136**, 9028-9035.

33. Z. Xiang, X. Zhou, C. Zhou, S. Zhong, X. He, C. Qin and D. Cao, *J. Mater. Chem.*, 2012, **22**, 22663-22669.